Relativistic structure of the deuteron: Electrodisintegration and *y* scaling

C. Ciofi degli Atti, D. Faralli, A. Yu. Umnikov, and L. P. Kaptari*
Department of Physics, University of Perugia and INFN, Sezione di Perugia, via A. Pascoli, Perugia, I-06100, Italy
(Received 15 September 1998; published 29 July 1999)

Realistic solutions of the spinor-spinor Bethe-Salpeter equation for the deuteron with the realistic interaction kernel, including the exchange of π, σ, ω, ρ, η, and δ mesons, are used to systematically investigate relativistic effects in inclusive quasielastic electron-deuteron scattering within the relativistic impulse approximation. Relativistic *y* scaling is considered by generalizing the nonrelativistic scaling function to the relativistic case, and it is shown that *y* scaling does occur in the usual relativistic scaling variable resulting from the energy conservation in the instant form of dynamics. The present approach of *y* scaling is fully covariant, with the deuteron being described by eight components, viz. the $^3S_1^{++}$, $^3S_1^{--}$, $^3D_1^{++}$, $^3D_1^{--}$, $^3P_1^{+-}$, $^3P_1^{-+}$, $^1P_1^{+-}$, $^1P_1^{-+}$ waves. It is demonstrated that if the negative relative energy states $^1P_1$, $^3P_1$ are disregarded, the concept of covariant momentum distributions $N(p_0,\mathbf{p})$, with $p_0=M_D/2-\sqrt{\mathbf{p}^2+m^2}$, can be introduced, and that calculations of electrodisintegration cross section in terms of these distributions agree within a few percent with the exact calculations, which include the $^1P_1$ and $^3P_1$ states, provided the nucleon three momentum $|\mathbf{p}|\leqslant 1$ GeV/*c*; in this momentum range, the asymptotic relativistic scaling function is shown to coincide with the longitudinal covariant momentum distribution. [S0556-2813(99)03708-5]

PACS number(s): 25.30.−c, 13.40.−f, 21.45.+v, 24.10.Jv

I. INTRODUCTION

The concept of scaling, which plays an important role in the investigation of the hadronic structure, can be introduced in the description of scattering processes whenever the cross section factorizes into a product of two different quantities, with the first one reflecting the nature of the scattering process, and therefore depending upon the relevant independent kinematical variables, and the second one (the *scaling function*) reflecting the internal structure of the target, and therefore depending upon a new variable (the *scaling variable*) which can be associated to the dynamics of the constituents of the target.

The best example of scaling (*x* scaling) is provided by inclusive deep inelastic scattering of leptons off nucleons [1]: in the Bjorken limit ($\nu\to\infty, Q^2\to\infty$, $x_{\rm Bj}=Q^2/2m\nu$ = const, with ν and Q^2 being, respectively, the energy and the four-momentum transfers, and m being the nucleon mass), the quantity $F_2(x_{\rm Bj},Q^2)\equiv\nu W_2^N(x_{\rm Bj},Q^2)$ where $W_2^N(x_{\rm Bj},Q^2)$ represents the deviation of the inclusive cross section from scattering off a pointlike nucleon, becomes Q^2 independent, i.e., scales in the variable $x_{\rm Bj}$ (the Bjorken scaling variable) which can be associated to the momentum fraction of the quark inside the hadron. Inclusive scattering of leptons off a nucleus A in the quasielastic (QE) region ($\nu\leqslant Q^2/2m$, i.e., $x_{\rm Bj}>1$) has been theoretically shown [2,4–6] to exhibit another kind of scaling, the so called *y* scaling, which can be summarized as follows:[1] at sufficiently high values of the three-momentum transfer $\mathbf{q}$, the quantity $|\mathbf{q}|W_{1(2)}^A(\nu,\mathbf{q}^2)/W_{1(2)}^N(\nu,\mathbf{q}^2)$, where the nuclear structure function $W_{1(2)}^A(\nu,\mathbf{q}^2)$ represents the deviation of the cross section from scattering off a pointlike nucleus, scales to a function of the variable *y*, according to $|\mathbf{q}|W_{1(2)}^A(\nu,\mathbf{q}^2)/W_{1(2)}^N(\nu,\mathbf{q}^2)\to F(y)$ where, in the case of the deuteron (but not for complex nuclei [5]), $F(y)$ represents the nucleon longitudinal momentum distribution $f(y)$:[2]

$$f(y)=\int_0^\infty n(p_\parallel,\mathbf{p}_\perp)d\mathbf{p}_\perp=2\pi\int_{|y|}^\infty n(\mathbf{p})|\mathbf{p}|d|\mathbf{p}|,\quad p_\parallel\equiv|y|. \tag{1.1}$$

Experimental data [6–8], due to the effect of the final-state interaction (FSI), exhibit only a qualitative scaling behavior, and a quantitative analysis [9] of deuteron data [8], taking into account the FSI, allowed one to obtain the nucleon momentum distribution in the deuteron using Eq. (1.1). It should, however, be stressed that the approach of Ref. [9], leading to Eq. (1.1), is based on a fully relativistic instant-form treatment of kinematics, but on the usual nonrelativistic (Schrödinger) treatment of the deuteron, and therefore lacks a consistent covariant treatment of the process.[3] Recently [11], a relativistic covariant model, based on the light-front dynamics and light cone kinematics [12], has been adopted to analyze inclusive QE scattering off the deuteron, treating

*On leave from Bogoliubov Lab. Theor. Phys., JINR, Dubna, Russia.

[1]For exhaustive reviews of *y* scaling see Refs. [2,3,5,6].

[2]We will consider, from now on, negative values of *y* for which the effects of non-nucleonic degrees of freedom are kinematically suppressed.

[3]Note that FSI have been treated in Ref. [9] within a full Schrödinger equation approach, i.e., using ground and continuum eigenfunctions of the same Hamiltonian. Such an approach is a correct one at the kinematics of the data of Ref. [8] which, at negative values of *y*, correspond to a very small (less than the pion threshold) relative energy of the neutron-proton pair in the continuum; it should always be kept in mind, however, that at high values of Q^2, such that the nucleon-nucleon (NN) cross section becomes strongly absorptive, the Schrödinger approach is inadequate (see, e.g., [10]).

the latter as a system of two spinless particles interacting via a simple scalar interaction. Within such a model, the deuteron wave function has only one component (the S wave), the square of which defines the model momentum distribution. However, it is well known that in the realistic case of two interacting spinor particles, the deuteron state is determined by at least four components if one nucleon is on-mass shell [13], five components within the spinor light cone formalism [14], or even eight components within the covariant Bethe-Salpeter (BS) approach [15,16].

The necessity of more than two components (S and D waves) in the description of the deuteron in a covariant approach, follows from an accurate account of the contribution of the negative relative energy states in the deuteron, the so-called P waves. Frequently, in the calculation of observables within covariant formalisms with realistic interactions, the final results are rather cumbersome (see, for instance, Refs. [13,17,18]) and a separation, in a compact form, of an analog of the momentum distribution of the deuteron becomes difficult, if not, sometimes, impossible. The inclusive quasielastic cross section and the concept of y scaling have not been so far considered within covariant approaches with realistic interaction, and an investigation of the possibility to define relativistic scaling functions and momentum distributions is still lacking.

In this paper we focus on a detailed study of quasielastic eD scattering, and the possibility of analyzing it in terms of scaling functions and momentum distributions, using the numerical BS solution recently obtained with a realistic one-boson exchange interaction [19–21].

Through this paper, as in [11], relativistic effects will be investigated within the impulse approximation (IA), which means that the final-state interaction of the np pair in the continuum will be disregarded, though it has been shown [9] that the FSI leads to sizable scaling violation effects at low values of $|\mathbf{q}|$. FSI effects will be analyzed in a subsequent paper [22], here we are only interested in the investigation of y scaling within a fully covariant treatment of inclusive eD scattering in IA, within a description of the deuteron in terms of realistic solutions of the BS equation.

Our paper is organized as follows: in Sec. II the derivation, within the BS formalism, of the two basic quantities which are necessary to define relativistic y scaling, i.e., the cross section for elastic electron scattering from a moving and off-mass-shell nucleon, and the cross section for inclusive quasielastic scattering from the deuteron, are presented; in Sec. III the relativistic scaling function is defined, its nonrelativistic reduction is illustrated, and the results of numerical calculations are presented; a relativistic momentum distribution appropriate to the BS approach is defined in Sec. IV, where the relationship between the relativistic momentum distribution and scaling function is illustrated; the summary and conclusions are presented in Sec. V; some relevant details concerning the construction of the Mandelstam vertex for the operator of eD scattering and for the computation of matrix elements within the Bethe-Salpeter formalism are given in Appendixes A and B, respectively.

II. THE ELECTRON-NUCLEON AND ELECTRON-DEUTERON CROSS SECTIONS WITHIN THE BETHE-SALPETER FORMALISM

A. General formulas for the cross section

In this section the cross sections for electron-hadron scattering within the covariant BS formalism will be derived. In particular, elastic scattering off a moving and off-mass-shell nucleon and inclusive quasielastic scattering off the deuteron at rest, will be considered. Both processes will be denoted $A(e,e')X$, where A stands for the target hadron and X for the final hadronic states. The four momenta of the initial and final electrons in the laboratory system are $k=(\mathcal{E},\mathbf{k})$ and $k'=(\mathcal{E}',\mathbf{k}')$, respectively; the four momentum transfer is $q=k-k'=(\nu,\mathbf{q})$, and the orientation of the coordinate system is defined by $\mathbf{q}=(0,0,q_z)$. At high energies the electron mass can be disregarded, so that

$$k^2=(k')^2\simeq 0, \quad kk'=-kq=\frac{-q^2}{2}=\frac{Q^2}{2}, \tag{2.1}$$

$$Q^2\equiv -q^2=4\mathcal{E}\mathcal{E}'\sin^2\frac{\theta}{2}, \tag{2.2}$$

where θ is the scattering angle. The following relations will be useful in what follows:

$$\mathcal{E}=\frac{\nu}{2}\left(1+\frac{\sqrt{\sin^2(\theta/2)+(Q^2/\nu^2)}}{\sin(\theta/2)}\right), \quad \mathcal{E}'=\mathcal{E}-\nu \tag{2.3}$$

$$\cos\theta_k=\frac{1}{\sqrt{1+Q^2/\nu^2}}\left(1+\frac{Q^2}{2\nu\mathcal{E}}\right), \tag{2.4}$$

$$|\mathbf{q}|=|q_z|=\sqrt{Q^2+\nu^2}, \tag{2.5}$$

where θ_k is the polar angle of the initial electron.

Hereafter the electron-nucleon vertex in the on-mass-shell form, viz:

$$\Gamma_\mu^{eN}(Q^2)=\gamma_\mu F_1(Q^2)+i\frac{\sigma_{\mu\alpha}q^\alpha}{2m}\kappa F_2(Q^2), \tag{2.6}$$

will be used, where $F_{1,2}$ are the electromagnetic form factors of the nucleon, and κ its anomalous magnetic moment. It is well known that the choice (2.6) for $\Gamma_\mu^{eN}(Q^2)$ violates gauge invariance; this is a relevant point which will be briefly discussed in Sec. III. In the one-photon exchange approximation the general formula for the invariant cross section for the process $A(e,e')X$ has the following form:

$$d\sigma=\frac{1}{4kp_A}|\mathcal{M}_{e+A\to e'+X}|^2(2\pi)^4 \times\delta^{(4)}(k+p_A-k'-p_X)\frac{d\mathbf{k}'}{(2\pi)^3 2\mathcal{E}'}d\tau_X, \tag{2.7}$$

where p_A is the initial target momentum, p_X is the total momentum of the final hadron state X, $d\tau_X$ is the phase space

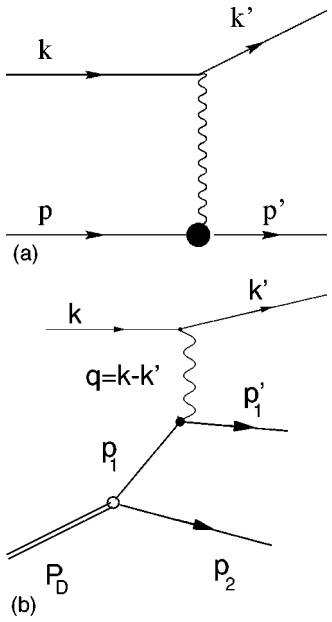

FIG. 1. Diagrams corresponding to elastic eN scattering (a), and inclusive eD scattering in the impulse approximation (b).

factor, and $\mathcal{M}_{e+A\to e'+X}$ is the invariant matrix element describing the process. For the elastic electron nucleon (eN) [Fig. 1(a)] and electron deuteron (eD) scattering in the impulse approximation [Fig. 1(b)], we have, respectively:

$$\left.\begin{aligned} &p_A=p, \quad p_X=p'=p+q,\\ &d\tau_X=\frac{d\mathbf{p}_1'}{(2\pi)^3 2E'} \end{aligned}\right\} \quad \text{for } eN \text{ scattering,} \tag{2.8}$$

$$\left.\begin{aligned} &p_A=P_D, \quad p_X=p_1'+p_2=P_D+q,\\ &d\tau_X=\frac{d\mathbf{p}_1'}{(2\pi)^3 2E_1'}\frac{d\mathbf{p}_2}{(2\pi)^3 2E_2}, \end{aligned}\right\} \quad \text{for } eD \text{ scattering.} \tag{2.9}$$

Using the identity

$$\frac{d\mathbf{p}_1'}{(2\pi)^3 2E_1'}=\delta((p_1')^2-m^2)\frac{d^4p_1'}{(2\pi)^3}, \tag{2.10}$$

the elastic eN and the inclusive eD cross sections are obtained by integrating over the d^4p_1':

$$\frac{d\sigma}{d\mathcal{E}'d\Omega_{k'}}=\frac{1}{4kp_A}\int |\mathcal{M}_{e+A\to e'+X}|^2(2\pi) \times\delta((p_1+q)^2-m^2)\frac{\mathcal{E}'}{2(2\pi)^3}d\tau, \tag{2.11}$$

where $d\tau$ is the phase space factor corresponding to the final hadron state X without the hit nucleon, $\Omega_{k'}$ is the scattered electron solid angle, and p_1 is the initial nucleon momentum in eN ($p_1^2=m^2$) and eD ($p_1=P_D-p_2$, $p_1^2\neq m^2$) scattering.

The square of the invariant matrix element in Eq. (2.11), averaged over the spins of the colliding particles and summed over the spins of the scattered particles, can be cast in the form

$$|\mathcal{M}_{e+A\to e'+X}|^2(2\pi)\delta((p_1+q)^2-m^2) =\frac{e^4}{Q^4}L^{\mu\nu}(k,q)W^A_{\mu\nu}(p_A,q), \tag{2.12}$$

where the leptonic tensor $L^{\mu\nu}$ has the familiar form:

$$L^{\mu\nu}(k,q)=2\left(2k_\mu k_\nu-(k_\mu q_\nu+k_\nu q_\mu)+g_{\mu\nu}\frac{q^2}{2}\right). \tag{2.13}$$

As for the hadronic tensor $W^N_{\mu\nu}$, appearing in elastic eN scattering, one has

$$W^N_{\mu\nu}(q^2,p_1\cdot q) =\tfrac{1}{2}\mathrm{Tr}\{(\hat{p}_1+m)\Gamma^{eN}_\mu(Q^2)(\hat{p}_1+\hat{q}+m)\Gamma^{eN}_\nu(Q^2)\} \times(2\pi)\delta((p_1+q)^2-m^2). \tag{2.14}$$

By contracting Eq. (2.14) with the leptonic tensor, Eq. (2.13), one obtains, in the nucleon rest system [$p_1=(m,\mathbf{0})$], the well-known Rosenbluth cross section. In the case of a complex system, e.g., the deuteron, only the general expression for the hadronic tensor can be unambiguously defined in terms of the two independent structure functions, $W_{1,2}(q^2,p_D\cdot q)$, whose explicit form, however, relies on particular theoretical models; the model adopted in this paper is described in the next subsection.

B. The hadronic tensor

Our strategy in computing the hadronic tensor for a composite system is the following one: a *nucleonic* tensor operator $\hat{O}^N_{\mu\nu}$ will be defined, whose expectation value between relativistic hadronic states $|A\rangle$ generates the corresponding hadronic tensor, according to

$$W^A_{\mu\nu}=\langle A|\hat{O}^N_{\mu\nu}|A\rangle. \tag{2.15}$$

The general requirements for the operator $\hat{O}^N_{\mu\nu}$ are as follows:

(i) it should lead to Eq. (2.14) when sandwiched between free nucleon states ($|A\rangle=|N\rangle$);

(ii) when sandwiched between deuteron states ($|A\rangle=|D\rangle$) it should incorporate the effects from the Fermi motion and the off-mass shellness of the hit nucleon.

The operator $\hat{O}_{\mu\nu}$, Eq. (2.15), due to the choice of the vertex (2.6), has the following form:

$$\hat{O}^N_{\mu\nu}(p_1,q)=(2\pi)\,\delta((p_1+q)^2-m^2)\Big\{F_1^2(Q^2)\hat{O}^{(1)}_{\mu\nu}(p_1,q)+\frac{\kappa}{2m}F_1(Q^2)F_2(Q^2)\hat{O}^{(12)}_{\mu\nu}(p_1,q)+\frac{\kappa^2}{4m^2}F_2^2(Q^2)\hat{O}^{(2)}_{\mu\nu}(p_1,q)\Big\}, \tag{2.16}$$

where

$$\hat{O}^{(1)}_{\mu\nu}(p_1,q)=2[-g_{\mu\nu}(\hat{p}_1+\hat{q}-m)+\gamma_\mu p_{1\nu}+\gamma_\nu p_{1\mu}], \tag{2.17}$$

$$\hat{O}^{(12)}_{\mu\nu}(p_1,q)=4[g_{\mu\nu}(-m\hat{q}+(q^2+qp_1))], \tag{2.18}$$

$$\hat{O}^{(2)}_{\mu\nu}(p_1,q)=2[g_{\mu\nu}(mq^2+\hat{p}_1q^2-\hat{q}(q^2+2qp_1))-q^2(\gamma_\mu p_{1\nu}+\gamma_\nu p_{1\mu})], \tag{2.19}$$

and all terms proportional to $q_{\mu(\nu)}$ have been omitted in view of the gauge invariance of the leptonic tensor (2.13), $q_{\mu(\nu)}L^{\mu\nu}=0$. In Eqs. (2.17)–(2.19) and in the rest of the paper the short-hand notation $\hat{p}$ will be used for the scalar product of a four-vector p with γ matrices, i.e., $\hat{p}\equiv\gamma_\mu p^\mu$. In actual calculations we first contract $\hat{O}^N_{\mu\nu}$ with the leptonic tensor $L^{\mu\nu}$, and the resulting operator is then sandwiched between target ground states. The result of the contraction is (see Appendix A):

$$\hat{O}(p_1,q,k)=L^{\mu\nu}\hat{O}_{\mu\nu}=\{\hat{O}_{\rm stat}+\delta\hat{O}_{\rm mot}+\delta\hat{O}_{\rm off}\}(2\pi)\times\delta((p_1+q)^2-m^2), \tag{2.20}$$

where

$$\hat{O}_{\rm stat}=2[q^2m-4m\nu\mathcal{E}+4m\mathcal{E}^2]A(Q^2)+\frac{q^4}{m}B(Q^2), \tag{2.21}$$

$$\delta\hat{O}_{\rm mot}=4[m\nu\mathcal{E}-\hat{q}(kp_1)-\mathcal{E}(2m\mathcal{E}-m\nu)+\hat{k}(2kp_1-qp_1)]A(Q^2), \tag{2.22}$$

$$\delta\hat{O}_{\rm off}\equiv-2q^2\left(\hat{q}+\frac{q^2}{2m}\right)F_1^2(Q^2)+\frac{2\kappa q^2}{m}(-m\hat{q}+qp_1)F_1(Q^2)F_2(Q^2)-\frac{\kappa^2q^2}{2m^2}[\hat{q}(q^2+2qp_1)]F_2^2(Q^2), \tag{2.23}$$

and

$$A(Q^2)\equiv\left(F_1^2(Q^2)-\frac{\kappa^2q^2}{4m^2}F_2^2(Q^2)\right), \tag{2.24}$$

$$B(Q^2)\equiv(F_1(Q^2)+\kappa F_2(Q^2))^2. \tag{2.25}$$

Let us discuss the meaning of the terms (2.21)–(2.23): $\hat{O}_{\rm stat}$ represents the contribution from the interaction of the lepton with the nucleon at rest, and in case of eN scattering its average over nucleon spinors yields the Rosenbluth cross section; $\delta\hat{O}_{\rm mot}$ originates the motion of the nucleon; $\delta\hat{O}_{\rm off}$ takes into account the off-mass shellness ($p_1^2\neq m^2$) of a bound nucleon, and therefore contributes only to the eD cross section.

As already pointed out, the eN and eD cross sections are obtained by sandwiching the relativistic operator $\hat{O}(p_1,q,k)$ between relativistic nucleon or deuteron states; this means that, within the present approach, the hadronic tensor has exactly the same form for a free or for a bound nucleon. The only assumption we make is that the electromagnetic vertices for free and bound nucleons are of the same form, with all nuclear effects provided by the state vectors. In the usual, noncovariant plane-wave impulse approximation (PWIA), based on the use of nonrelativistic wave functions, the cross section off a nucleus A is obtained by relating the nuclear hadronic tensor $W^A_{\mu\nu}$ to the nucleon hadronic tensor $W^N_{\mu\nu}$ by a convolution formula, with resulting ambiguities as far as the extrapolation of the eN cross section for a bound off-mass shell nucleon is concerned (see, e.g., [23,24]).

As previously mentioned, gauge invariance is broken for the deuteron current corresponding to the choice Eq. (2.16). Several phenomenological prescriptions have been, however, suggested to restore it [23,24]. It should be pointed out that our paper is mainly aimed at theoretically comparing relativistic and nonrelativistic deuteron momentum distributions and y-scaling functions, without presenting any comparison with experimental data which would, of course, require a serious consideration of gauge invariance violation effects.

The procedure used in this paper can, in principle, be adopted in the description of eD scattering within the nonrelativistic, Schrödinger picture. However, in this case, consistency would require a nonrelativistic reduction of the γNN vertex. A systematic study of deuteron electrodisintegration within the nonrelativistic approach taking into account the FSI, relativistic corrections, and meson exchange currents, can be found in [25] and references quoted therein.

C. The elastic electron-nucleon cross section

The elastic eN cross section resulting by sandwiching $\hat{O}_{\rm stat}$ and $\delta\hat{O}_{\rm mot}$ between free nucleon states reads as follows:

$$\frac{d\sigma}{d\Omega_{k'}}=\frac{\mathcal{E}E_{\vec{p}_1}}{(p_1k)}f_{\rm recoil}\widetilde{\sigma^{eN}}, \tag{2.26}$$

where (i) $f_{\rm recoil}$ is the recoil term

$$f^{-1}_{\rm recoil}=1+\frac{2\mathcal{E}\sin^2\theta/2-\nu}{E_{\vec{p}_1+\vec{q}}}-\frac{p_{1z}}{|\mathbf{q}|}\frac{\nu-2\mathcal{E}\sin^2\theta/2}{E_{\vec{p}_1+\vec{q}}}. \tag{2.27}$$

(ii) $\mathcal{E}E_{\vec{p}_1}/(p_1k)$ comes from the redefinition of the incident flux for a moving nucleon; (iii) $\widetilde{\sigma^{eN}}$ is the ''reduced''

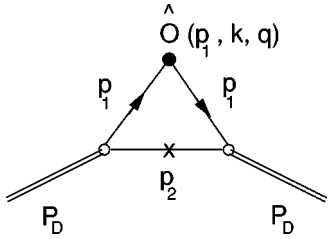

FIG. 2. The diagram corresponding to the averaging of the operator $\hat{O}$, Eq. (2.20), between deuteron states. The crossed line corresponds to the nucleon on the mass shell.

electron-nucleon cross section, i.e., the cross section without the flux factor and the recoil contribution,

$$\widetilde{\sigma^{eN}}=\sigma_{\rm Mott}\frac{m^2}{E_{\vec{p}_1}E_{\vec{p}_1+\vec{q}}}\left\{A(Q^2)+\frac{Q^2}{2m^2}\tan^2\frac{\theta}{2}B(Q^2)+\frac{A(Q^2)}{m^2\mathcal{E}\mathcal{E}'\cos^2\theta/2}[(p_1k)^2-(p_1k)(p_1q)-m^2\mathcal{E}\mathcal{E}']\right\}, \tag{2.28}$$

where

$$\sigma_{\rm Mott}\equiv\frac{\alpha^2\cos^2(\theta/2)}{4\mathcal{E}^2\sin^4(\theta/2)} \tag{2.29}$$

is the Mott cross section. In the above equation $E_{\vec{p}_1}=\sqrt{m^2+\mathbf{p}_1^2}$, $E_{\vec{p}_1+\vec{q}}=\sqrt{m^2+(\mathbf{p}_1+\mathbf{q})^2}$. It can easily be seen from Eqs. (2.26)–(2.28) that for a nucleon at rest $[p_1=(m,\mathbf{0})]$ Eq. (2.26) coincides with the Rosenbluth cross section.

D. The inclusive electron-deuteron cross section within the BS formalism

The *relativistic impulse approximation* for the inclusive eD cross section is obtained by averaging the operator $\hat{O}$, given by Eq. (2.20), with the Bethe-Salpeter amplitudes (see Fig. 2). The result is

$$\left(\frac{d\sigma}{d\mathcal{E}'d\Omega_{k'}}\right)_{eD}^{\rm BS}=\sigma_{\rm Mott}\int_{|y|}^{p_{\max}}\frac{|\mathbf{p}|^2d|\mathbf{p}|}{(2\pi)^4}\frac{1}{16\mathcal{E}\mathcal{E}'\cos^2(\theta/2)}\int_0^{2\pi}\frac{d\varphi_p}{|\mathbf{p}|\cdot|\mathbf{q}|}\frac{1}{2wM_D}\frac{1}{[M_D(M_D-2w)]^2}\times\left[\frac{1}{3}\sum_M{\rm Tr}\{\bar{G}_M(p,P_D)(\hat{p}_1+m)(\hat{O}_{\rm stat}+\delta\hat{O}_{\rm mot}+\delta\hat{O}_{\rm off})(\hat{p}_1+m)G_M(p,P_D)(\hat{p}_2+m)\}\right], \tag{2.30}$$

where $p_1=P_D-p_2$, G_M is the Bethe-Salpeter $D\to NN$ vertex, M is the deuteron total angular momentum projection, p is the relative momentum of the nucleons, i.e., $p_{1,2}=P_D/2\pm p$. The deuteron-nucleon vertex G_M is the truncated Green's function which is related to the conjugated Bethe-Salpeter amplitude Ψ_M by

$$\Psi_M(p,P_D)=\frac{(\hat{p}_1+m)}{(p_1^2-m^2)}G_M(p,P_D)\frac{(\hat{p}_2+m)}{(p_2^2-m^2)}. \tag{2.31}$$

The limits of integration in Eq. (2.30), $|\mathbf{p}|_{\min}\equiv|y|$ and $p_{\max}$ are obtained from energy conservation provided by the δ function

$$\delta((P_D-p_2+q)^2-m^2)=\frac{1}{2|\mathbf{p}|\cdot|\mathbf{q}|}\delta\left(\cos\theta_p-\frac{M_D(M_D+2\nu)+q^2-2w(M_D+\nu)}{2|\mathbf{p}|\cdot|\mathbf{q}|}\right), \tag{2.32}$$

which determines the value of $\cos\theta_p$ from the constraint:

$$-1\leqslant\cos\theta_p\leqslant 1. \tag{2.33}$$

Solving the inequalities (2.33) with $\cos\theta_p$ defined by the argument of the δ function (2.32), we obtain the same result as in [9], i.e.,

$$|\mathbf{p}|_{\min}=\frac{1}{2}\left|\left\{(M_D+\nu)\sqrt{1-\frac{4m^2}{s}}-|\mathbf{q}|\right\}\right|\equiv|y|, \tag{2.34}$$

$$|\mathbf{p}|_{\max}=\frac{1}{2}\left\{(M_D+\nu)\sqrt{1-\frac{4m^2}{s}}+|\mathbf{q}|\right\}\equiv p_{\max}, \tag{2.35}$$

where s denotes the Mandelstam variable for the γ^*D vertex

$$s=(P_D+q)^2=M_D(M_D+2\nu)-Q^2. \tag{2.36}$$

It can be seen from Eq. (2.35) that $p_{\max}$ sharply increases with $|\mathbf{q}|$, such a circumstance, as we shall see, has relevant consequences for the occurrence of y scaling.

In the calculation of the trace appearing in Eq. (2.30), two different operators have to be considered, namely the scalar operator, $\hat{\mathbf{1}}$, coming from $\hat{O}_{\rm stat}$ [Eq. (2.21)], and the vector operator γ_μ, contained in $\delta\hat{O}_{\rm mot}$ and $\delta\hat{O}_{\rm off}$, [Eqs. (2.22) and (2.23)].

We have calculated the BS average of these operators, $\langle\hat{\mathbf{1}}\rangle_{\rm pole}$ and $\langle\gamma_\mu\rangle_{\rm pole}$, where the subscript ''pole'' means that the trace in Eq. (2.30) has been obtained using Eq. (2.31) and by evaluating the integral over p_{20} in the pole corresponding to the second particle on-mass shell (for details, see Appendix B), i.e.,

$$p_{20}=w=\sqrt{\mathbf{p}^2+m^2},\quad p_0=\frac{M_D}{2}-w,\quad p_{10}=M_D-w. \tag{2.37}$$

The eD cross section can now be rewritten in terms of the nucleon pole contributions to the vector and the scalar parts, namely,

$$\left(\frac{d\sigma}{d\mathcal{E}'d\Omega_{k'}}\right)^{\rm BS}_{eD}=\sigma_{\rm Mott}(2\pi)\int_{|y|}^{p_{\rm max}}\frac{|\mathbf{p}|^2d|\mathbf{p}|}{(2\pi)^4}\times\frac{1}{8\mathcal{E}\mathcal{E}'\cos^2(\theta/2)}\int_0^{2\pi}\frac{d\varphi_p}{2|\mathbf{p}|\cdot|\mathbf{q}|}\times(f_{\rm stat}+\delta f_{\rm mot}+\delta f_{\rm off}), \tag{2.38}$$

where

$$f_{\rm stat}=\left[2m[q^2+4\mathcal{E}\mathcal{E}']A(Q^2)+\frac{q^4}{m}B(Q^2)\right]\langle\hat{\mathbf{1}}\rangle^{\rm BS}_{\rm pole}(\mathbf{p}), \tag{2.39}$$

$$\delta f_{\rm mot}=4\{-2m\mathcal{E}\mathcal{E}'\langle\hat{\mathbf{1}}\rangle^{\rm BS}_{\rm pole}(\mathbf{p})+[-q^\mu(kp_1)+k^\mu(2kp_1-qp_1)]\langle\gamma_\mu\rangle^{\rm BS}_{\rm pole}(\mathbf{p})\}A(Q^2), \tag{2.40}$$

$$\delta f_{\rm off}=-2q^2\left[q^\mu\langle\gamma_\mu\rangle^{\rm BS}_{\rm pole}(\mathbf{p})+\frac{q^2}{2m}\langle\hat{\mathbf{1}}\rangle^{\rm BS}_{\rm pole}(\mathbf{p})\right]F_1^2(Q^2)+\frac{2\kappa q^2}{m}[-mq^\mu\langle\gamma_\mu\rangle^{\rm BS}_{\rm pole}(\mathbf{p})+qp_1\langle\hat{\mathbf{1}}\rangle^{\rm BS}_{\rm pole}(\mathbf{p})]F_1(Q^2)F_2(Q^2)-\frac{\kappa^2q^2}{2m^2}[q^\mu\langle\gamma_\mu\rangle^{\rm BS}_{\rm pole}(\mathbf{p})(q^2+2qp_1)]F_2^2(Q^2). \tag{2.41}$$

Let us compare Eq. (2.38), which represents the BS eD inclusive cross section in which the matrix elements of both the eN and the $D\to NN$ vertices are treated covariantly, with the usual noncovariant PWIA cross section, where the eN vertex is treated covariantly within the instant-form of dynamics, and the vertex $D\to NN$ is treated noncovariantly within the Schrödinger approach, viz.

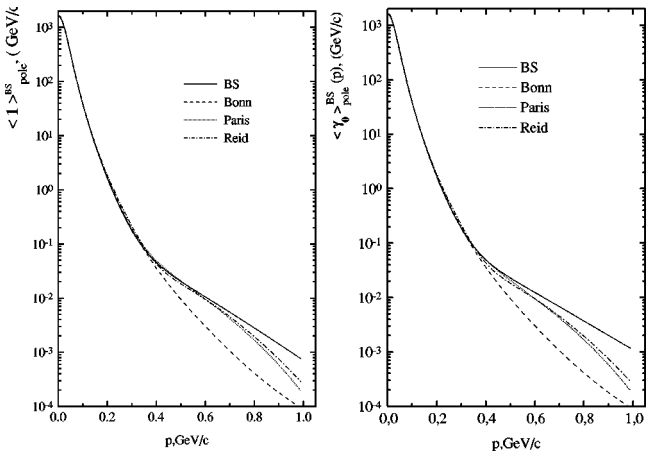

FIG. 3. The Bethe-Salpeter matrix elements $\langle\mathbf{1}\rangle^{\rm BS}_{\rm pole}(\mathbf{p})$ and $\langle\gamma_0\rangle^{\rm BS}_{\rm pole}(\mathbf{p})$ (solid lines) compared with their nonrelativistic limits, Eq. (2.44), computed with nucleon momentum distribution $n_D(\mathbf{p})$ corresponding to the realistic Bonn [27] (dashed), Paris [28] (dotted), and Reid [29] (dash-dotted) interactions.

$$\left(\frac{d\sigma}{d\mathcal{E}'d\Omega_{k'}}\right)^{\rm PWIA}_{eD}=(2\pi)\int_{|y|}^{p_{\rm max}}|\mathbf{p}|d|\mathbf{p}|n_D(\mathbf{p})\frac{E_{\vec{p}+\vec{q}}}{|\mathbf{q}|}\times(\bar{\sigma}_{ep}+\bar{\sigma}_{en}), \tag{2.42}$$

where $\bar{\sigma}_{ep(n)}$ is the relativistic electron-nucleon cross section for a free moving nucleon (see, e.g., Ref. [23]) and the nonrelativistic momentum distribution $n_D(\mathbf{p})$ is normalized as follows:

$$\int d\mathbf{p}\,n_D(\mathbf{p})=1. \tag{2.43}$$

The most relevant difference between Eqs. (2.38) and (2.42) arises from the noncovariant treatment of the $D\to NN$ vertex which, in Eq. (2.42), is entirely determined by a single quantity, the nucleon momentum distribution $n_D(\mathbf{p})$, whereas in the covariant BS cross section, Eq. (2.38), it depends upon $\langle\hat{\mathbf{1}}\rangle^{\rm BS}_{\rm pole}$ and $\langle\gamma_\mu\rangle^{\rm BS}_{\rm pole}$. In order to exhibit the quantitative difference between the two cross sections let us compare $\langle\hat{\mathbf{1}}\rangle^{\rm BS}_{\rm pole}$ and $\langle\gamma_\mu\rangle^{\rm BS}_{\rm pole}$ with their nonrelativistic limits ($|\mathbf{p}|^2/m^2\ll1$) which are given by (for details see Refs. [19,26]):

$$\langle\gamma_\mu\rangle^{\rm BS}_{\rm pole}(\mathbf{p})\to(2\pi)^3(p_\mu/E_{\mathbf{p}})n_D(\mathbf{p}),$$

$$\langle\mathbf{1}\rangle^{\rm BS}_{\rm pole}(\mathbf{p})\to(2\pi)^3(m/E_{\mathbf{p}})n_D(\mathbf{p}), \tag{2.44}$$

where $p_\mu=(E_{\mathbf{p}},\mathbf{p})$ and $n_D(\mathbf{p})$ is the deuteron momentum distribution.

In Figs. 3 and 4 $\langle\hat{\mathbf{1}}\rangle^{\rm BS}_{\rm pole}$ and $\langle\gamma_\mu\rangle^{\rm BS}_{\rm pole}$ are compared with their nonrelativistic limit obtained with $n_D(\mathbf{p})$ corresponding to various realistic interactions. Using Eqs. (2.44) the nonrelativistic limit of the BS cross section can be obtained straightforwardly, viz.

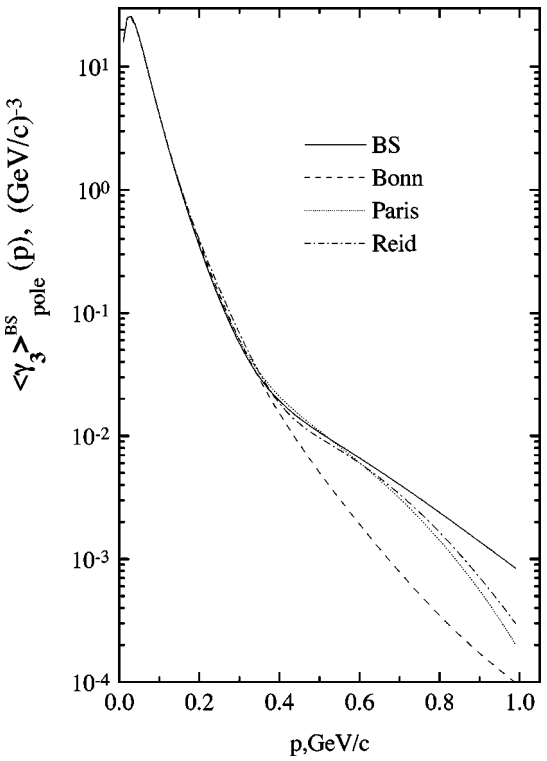

FIG. 4. The same as in Fig. 3 but for the vector density $\langle \gamma_3 \rangle^{\rm BS}_{\rm pole}(\mathbf{p})$ corresponding to $\cos\theta_{\hat{p}\hat{q}}=1$.

$$\left(\frac{d\sigma}{d\mathcal{E}'d\Omega_{k'}}\right)^{\rm NR}_{eD}=(2\pi)\int_{|y|}^{p_{\max}}|\mathbf{p}|d|\mathbf{p}|n_D(\mathbf{p})\frac{E_{\vec{p}+\vec{q}}}{|\mathbf{q}|}(\tilde{\sigma}_{ep}+\tilde{\sigma}_{en}), \tag{2.45}$$

where $\tilde{\sigma}_{eN}=\tilde{\sigma}_{eN}(|\mathbf{p}|,|\mathbf{q}|,\nu)$ is given by Eq. (2.28), without the off-mass shell contribution [Eq. (2.41)], which can easily be shown to vanish in the nonrelativistic limit.

Thus, we have demonstrated that the nonrelativistic limit of the BS inclusive cross section (2.38), obtained by taking the nonrelativistic limit of $\langle \hat{\mathbf{1}} \rangle^{\rm BS}_{\rm pole}$ and $\langle \gamma_\mu \rangle^{\rm BS}_{\rm pole}$, has exactly the same structure as the instant form result of Ref. [5], apart from some minor differences between the relativistic eN cross sections $\tilde{\sigma}_{eN}$ and $\bar{\sigma}_{eN}$, which are irrelevant for the present paper, and which will be discussed elsewhere [22].

In closing this section, the following remarks are in order: (i) the BS covariant inclusive eD cross section does not factorize into a product of an electron nucleon cross section and a deuteron structure function. In this respect the covariant results differ from the usual noncovariant PWIA; (ii) within the BS formalism the interacting nucleon is consistently treated as an off-mass shell particle. Consequently, the matrix element of the γNN vertex is half off shell for the eD scattering. As a result, additional off-mass shell effects, represented by Eq. (2.41), arise due to covariance of the approach.

III. THE RELATIVISTIC SCALING FUNCTION

A. Nonrelativistic and relativistic scaling functions

In the nonrelativistic case, the concept of y scaling can be introduced when the value of $|\mathbf{q}|$ becomes large enough so as to make $p_{\max}\sim\infty$ and the dependence of $\bar{\sigma}_{eN}$ (or $\tilde{\sigma}_{eN}$) upon $|\mathbf{p}|$ very weak. In such a case, Eq. (2.45) can be cast in the following form:

$$\left(\frac{d\sigma}{d\mathcal{E}'d\Omega_{k'}}\right)^{\rm NR}_{eD}=(s_{ep}+s_{en})\frac{E_{y+|\vec{q}|}}{|\mathbf{q}|}(2\pi)\int_{|y|}^{\infty}|\mathbf{p}|d|\mathbf{p}|n_D(\mathbf{p}), \tag{3.1}$$

where s_{eN} and $E_{y+|\vec{q}|}$ represent $\tilde{\sigma}_{eN}$ and $E_{\vec{p}+\vec{q}}$, calculated at $|\mathbf{p}|=|\mathbf{p}|_{\min}=|y|$ and are taken out of the integral. Such an approximation has been carefully investigated in Ref. [5] and found to be valid within few percents, provided $Q^2>0.5$ GeV$^2/c^2$. It is clear therefore, that at large values of $|\mathbf{q}|$ the following quantity (the nonrelativistic scaling function)

$$F^{\rm NR}(|\mathbf{q}|,y)\equiv\frac{|\mathbf{q}|}{E_{y+|\vec{q}|}}\cdot\left(\frac{d\sigma}{d\mathcal{E}'d\Omega_{k'}}\right)^{\rm NR}_{eD}\Big/(s_{ep}+s_{en}) \tag{3.2}$$

will be directly related to the longitudinal momentum distribution [5]

$$F^{\rm NR}(|\mathbf{q}|,y)\to f(y)=2\pi\int_{|y|}^{\infty}|\mathbf{p}|d|\mathbf{p}|n_D(|\mathbf{p}|), \tag{3.3}$$

whose first derivative will provide the nonrelativistic momentum distribution. As already pointed out, the condition for the occurrence of nonrelativistic y scaling is that Eq. (2.45) could be cast in the form (3.1), which means that (i) $Q^2>0.5$ GeV$^2/c^2$, in order to make the replacement $\tilde{\sigma}_{eN}\to s_{eN}$ and $E_{\vec{p}+\vec{q}}\to E_{y+|\vec{q}|}$ possible, and (ii) $p_{\max}=(|\mathbf{q}|-|y|)\gg|y|$ [cf. Eqs. (2.34) and (2.35)] in order to saturate the integral of the momentum distribution, $\int_{|y|}^{p_{\max}}|\mathbf{p}|d|\mathbf{p}|n_D(|\mathbf{p}|)\to\int_{|y|}^{\infty}|\mathbf{p}|d|\mathbf{p}|n_D(|\mathbf{p}|)$. Condition (ii) obviously implies that the larger the value of $|y|$, the larger the value of $|\mathbf{q}|$ at which scaling will occur. The satisfaction of the inequalities $|\mathbf{q}|\gg2|y|, x_{\rm Bj}>1$ lead, for any well-behaved $n_D(|\mathbf{p}|)$, to the following conditions for the occurrence of nonrelativistic y scaling:

$$2m/3\leqslant\nu<|\mathbf{q}|, \quad |\mathbf{q}|\geqslant2m. \tag{3.4}$$

Note, that the above conditions are very different from the conditions for Bjorken scaling $\nu\simeq|\mathbf{q}|$. Let us now discuss relativistic scaling. To keep contact with nonrelativistic scaling, let us define the following relativistic scaling function:

$$F^{\rm BS}(|\mathbf{q}|,y)\equiv\frac{|\mathbf{q}|}{E_{y+|\vec{q}|}}\cdot\left(\frac{d\sigma}{d\mathcal{E}'d\Omega_{k'}}\right)^{\rm BS}_{eD}\Big/(s_{ep}+s_{en}), \tag{3.5}$$

with $(d\sigma/d\mathcal{E}'d\Omega_{k'})^{\rm BS}_{eD}$ given by Eq. (2.38). In the rest of the paper the following questions will be answered:

(i) Does (and at which values of $|\mathbf{q}|$) Eq. (3.5) scale in y?

(ii) If scaling does occur, can a relationship be established between the asymptotic scaling function and the momentum distribution?

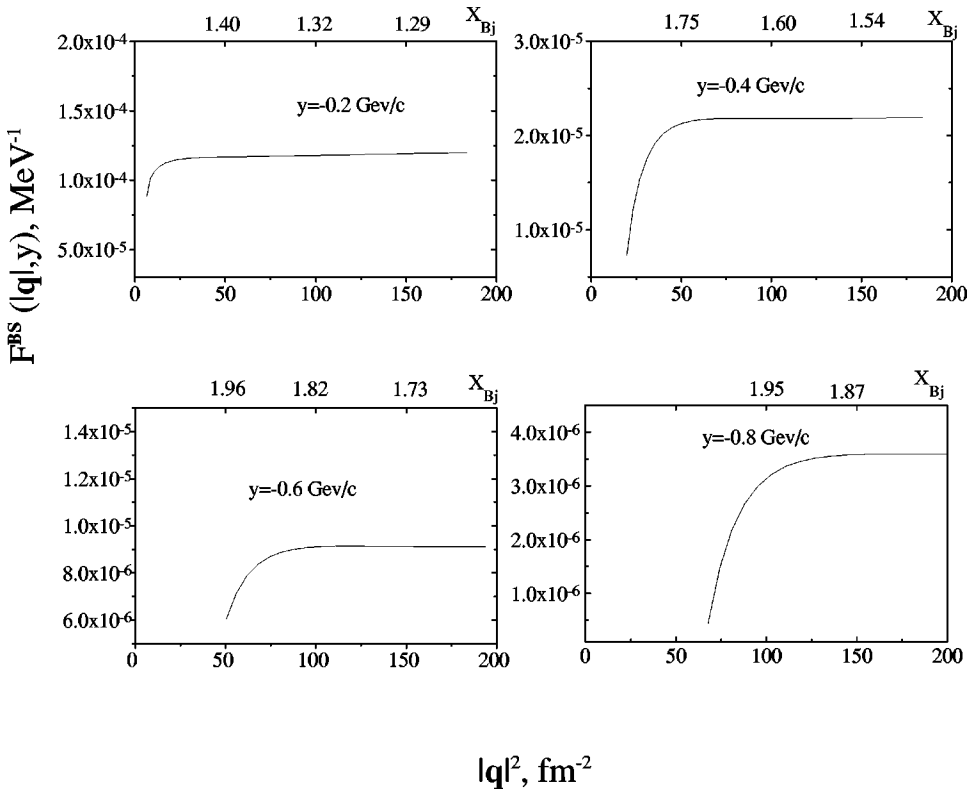

FIG. 5. The scaling function $F^{\mathrm{BS}}(|\mathbf{q}|,y)$, Eq. (3.5) vs $|\mathbf{q}|^2$ for various values of y. For the sake of completeness, the value of the Bjorken variable $x_{\mathrm{Bj}}=Q^2/2m\nu$ is also shown.

It is clear, by looking at Eq. (2.38), that relativistic scaling, as the nonrelativistic one, is entirely governed by the value of $p_{\max}$ [Eq. (2.35)], in that one expects that, starting from a certain high value of $|\mathbf{q}|$, $p_{\max}$ becomes large enough as to saturate the $|\mathbf{p}|$ dependence of $\langle\hat{\mathbf{1}}\rangle_{\mathrm{pole}}(|\mathbf{p}|)$ and $\langle\gamma_\mu\rangle_{\mathrm{pole}}(|\mathbf{p}|)$. It should be pointed out that if scaling of Eq. (3.5) is observed, this would imply that a factorization of Eq. (2.38) similar to the one occurring in the nonrelativistic case [i.e., Eq. (3.2)] occurs in the relativistic case as well. Such a factorization, due to the complex structure of Eq. (2.38) is, *a priori*, not obvious. As for the second question, it is by no means a trivial one, for in the BS case even the concept of momentum distributions is not well defined. Nevertheless, we will see that the concept of relativistic momentum distributions can be introduced, and that a relationship of such a momentum distribution with the asymptotic scaling function, can be established.

B. Numerical calculations of the relativistic cross section and scaling function

In this section the results of numerical calculations of the relativistic scaling function $F^{\mathrm{BS}}(|\mathbf{q}|,y)$, Eq. (3.5), will be presented. In our calculations the numerical solution [19,21] of the spinor-spinor BS equation containing a realistic one-boson-exchange interaction kernel, which includes the set of π, σ, ω, ρ, η, and δ exchanged mesons, is used. The meson parameters (masses, coupling constants, and cutoff parameters) have been taken to be the same as in Refs. [15,16], except for the coupling constant of the scalar σ meson, which has been adjusted to provide a numerical solution of the homogeneous BS equation. Recently, the solution became available in the form of analytical parametrizations obtained by fitting the numerical solution to the BS equation, using the least-squares procedure [20]. The details of numerical calculation of various matrix elements appearing in eD electrodisintegration are given in Appendix B.

In Fig. 5 the approach to scaling of the BS scaling function (3.5) is shown for various values of y. It can be seen that scaling is approached very rapidly due to the sharp increase of $p_{\max}$ in Eq. (2.38) with $|\mathbf{q}|$ (cf. Fig. 6). It can also be seen that the value of $|\mathbf{q}|$, at which scaling is reached, sharply increases with the value of y, going from $|\mathbf{q}|\sim 1$ GeV/c ($\nu\sim 0.3$ GeV), at $y=-0.2$ GeV/c, to $|\mathbf{q}|\sim 2$ GeV/c ($\nu\sim 0.8$ GeV) at $y=-0.8$ GeV/c. These values match very well the condition for nonrelativistic y scaling (3.4); this apparently surprising result will be explained later on. Let us now briefly discuss the role played by inelastic channels on the scaling function. It can be shown [22] that for all values of y presented in Fig. 5, the values of ν and $|\mathbf{q}|$ in the region of the approach to scaling are below the pion production threshold, which can be reached only at higher values of $|\mathbf{q}|$, provided $Q^2\leqslant 5$ GeV$^2/c^2$. Therefore, inelastic excitations of the nucleon are kinematically forbidden in a wide range of $|\mathbf{q}|$ for a given value of y. The asymptotic scaling function is shown vs. y in Fig. 7, whereas the contribution of the off-mass shell terms (2.41) is presented in Fig. 8. By comparing the two figures, it can be seen that the off-mass shell corrections are negligibly small in the

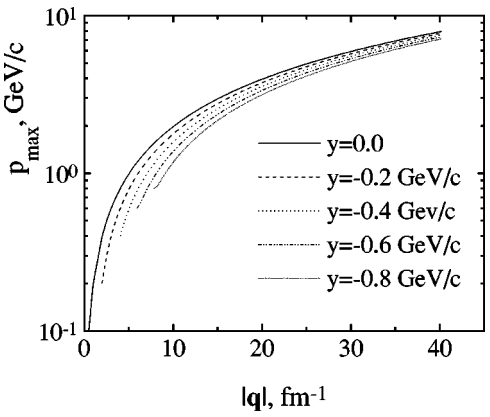

FIG. 6. The dependence of the upper limit of integration $|\mathbf{p}|_{\max}$ in Eq. (2.35) upon $|\mathbf{q}|$, for fixed values of y.

whole range of $|y|$, and in what follows they will be disregarded. Figure 9 illustrates the role of the ''moving'' components, Eq. (2.40), calculated at different values of $|\mathbf{q}|=3$, 10, and 18 GeV/c; as expected, these corrections increase with $|y|$ and are practically $|\mathbf{q}|$ independent. The various contributions to the total scaling function are presented in Fig. 10, whereas, in Fig. 11 the asymptotic relativistic BS scaling function is compared with the nonrelativistic one, calculated with various realistic interactions. It can be seen that for $|y|>0.4$ GeV/c, the differences between the BS and the nonrelativistic scaling functions are very large, except for the Reid soft core interaction.

The scaling behavior of the relativistic scaling function (3.5) shown in Fig. 5 would imply the factorization of the BS

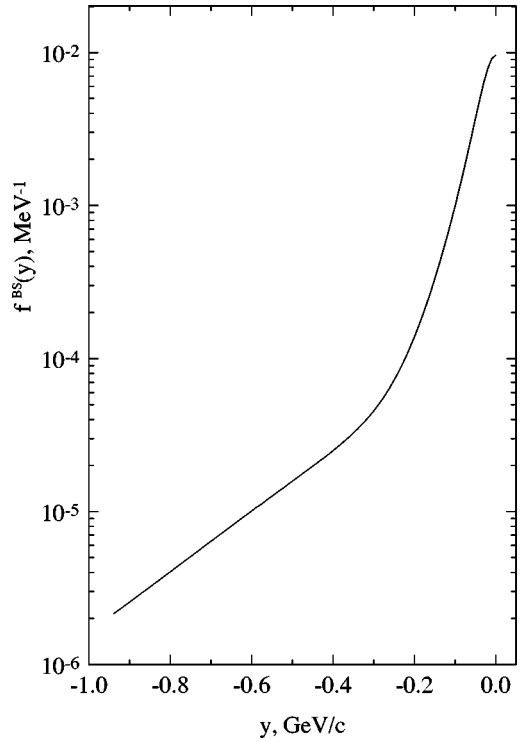

FIG. 7. The asymptotic scaling function $f^{\mathrm{BS}}(y)$ computed within the Bethe-Salpeter formalism [Eq. (3.5) evaluated at $|\mathbf{q}|\rightarrow\infty$].

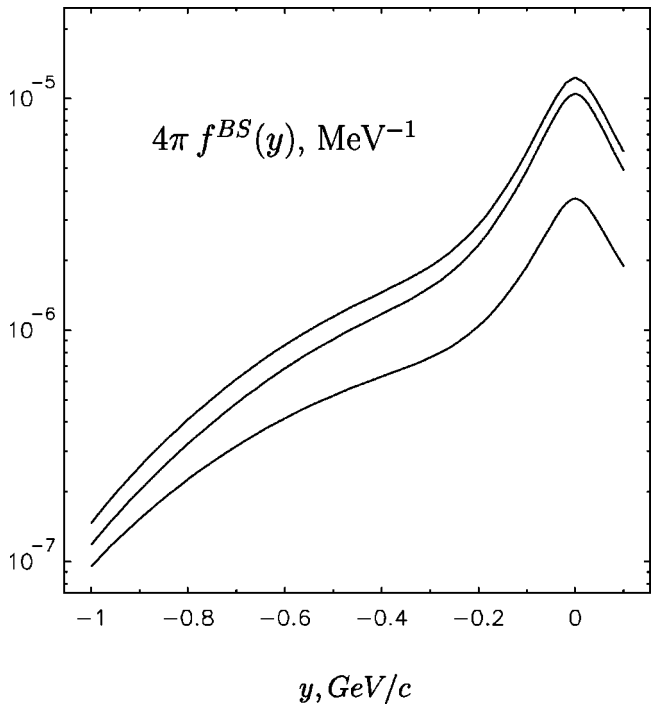

FIG. 8. Off-mass-shell contributions to $f^{\mathrm{BS}}(y)$: the three curves correspond (from the top) to the three terms of Eq. (2.41).

inclusive cross section (2.38) into the free eN cross section and some kind of deuteron structure function. Due to the complexity of Eqs. (2.39)–(2.41), neither the origin of such a factorization, nor the nature of the deuteron structure function are clear at the moment; they will, however, be discussed and clarified in the next section.

IV. RELATIVISTIC MOMENTUM DISTRIBUTION

Since in the covariant BS formalism the deuteron amplitude does not have a probabilistic interpretation, the concept

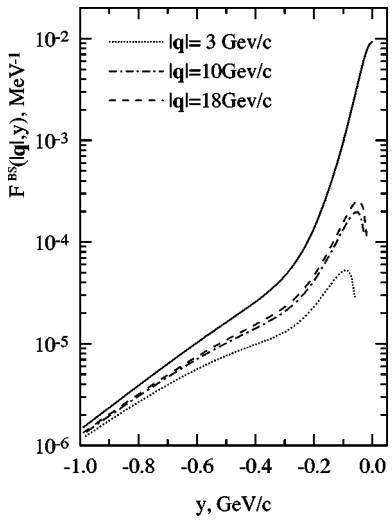

FIG. 9. The ''moving corrections'' to $F^{\mathrm{BS}}(|\mathbf{q}|,y)$, Eq. (2.40), for $|\mathbf{q}|=3$, 10, and 18 GeV/c, respectively. The solid line is the asymptotic scaling function $f^{\mathrm{BS}}(y)$.

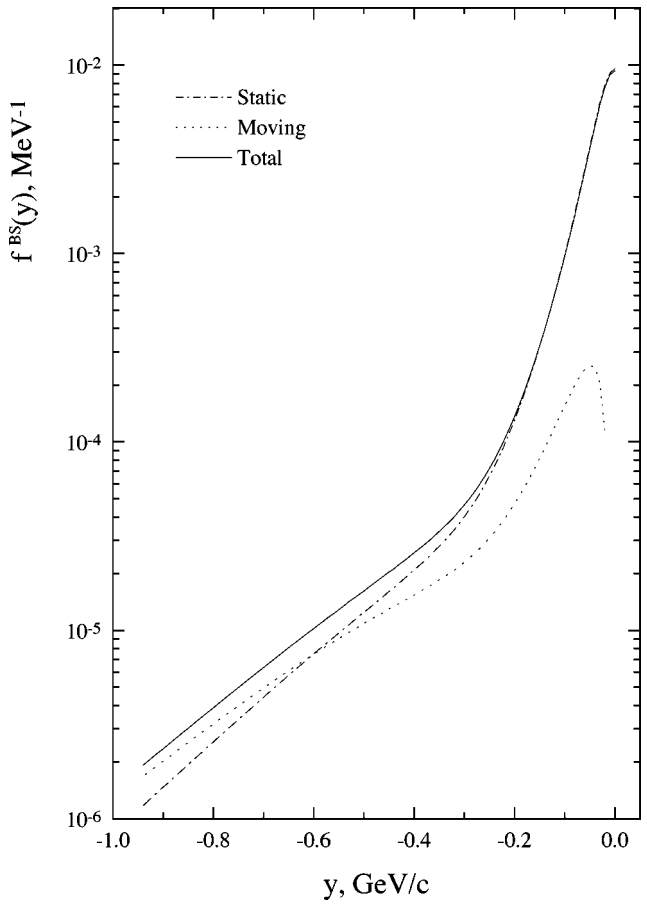

FIG. 10. The various contributions to the asymptotic scaling function $f^{\mathrm{BS}}(y)$. Dot-dashed line: the static part (2.39); dotted line: the ''moving'' corrections (2.40). The solid line is the total scaling function [Eq. (3.5) evaluated at $|\mathbf{q}|\to\infty$].

of momentum distribution is ambiguous. Nevertheless, we will now rearrange the matrix elements of $\hat{\mathbf{1}}$ and γ_μ in such a way that, under certain conditions, they could be interpreted in terms of a relativistic momentum distribution.

Let us return to the main quantity, Eq. (2.30), and try to analyze it analytically in more detail. To this end, it is convenient in the decomposition of the BS amplitude to shift from the Dirac basis, used in Ref. [19], to a basis of spin-angular matrices [15,30], i.e., an outer product of two spinors, representing the solutions of the free Dirac equation with positive and negative energies. This basis, which is frequently used, is labeled by the relative momentum $\vec{p}$, the helicities λ_i, and the energy spin ρ_i of the particles [15], and is sometimes called the $(J,\lambda_1,\lambda_2,\rho_1,\rho_2)$ representation. The spectroscopic notations are used for the partial amplitudes viz. $^{2S+1}L_J^{\rho_1,\rho_2}$, i.e.,

$$^3S_1^{++},{}^3S_1^{--},{}^3D_1^{++},{}^3D_1^{--},{}^1P_1^{+-},{}^1P_1^{-+},{}^3P_1^{+-},{}^3P_1^{-+}. \tag{4.1}$$

The partial amplitudes in the basis (4.1) exhibit a more transparent physical meaning, since they can be compared with the deuteron states in the nonrelativistic limit. It is intuitively clear that the two nucleons in the deuteron are mainly in

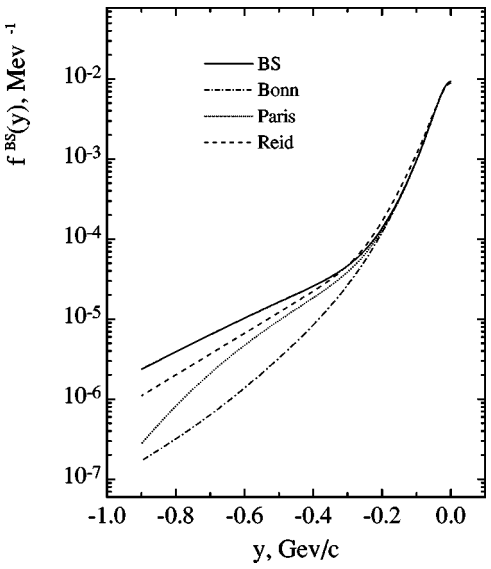

FIG. 11. The BS asymptotic scaling function (full) compared with the nonrelativistic scaling function (3.2) corresponding to the Reid (dashed), Paris (dotted), and Bonn (dot-dashed) interactions.

positive energy states with $L=0,2$, so that one may expect the probability of negative energy states with $L=1$ in Eq. (4.1) to be much smaller than the probability for the $^3S_1^{++}$ and $^3D_1^{++}$ states. Moreover, it can be shown that the waves $^3S_1^{++}$ and $^3D_1^{++}$ directly correspond to the S and D waves in the deuteron, with the waves with negative energy vanishing in the nonrelativistic limit. (The connection between the partial amplitudes defined in the Dirac and the ρ-spin representation can be found in Ref. [18].)

Let us now investigate analytically the matrix elements $\langle\gamma_\mu\rangle^{\mathrm{BS}}_{\mathrm{pole}}(\mathbf{p})$ and $\langle\mathbf{1}\rangle^{\mathrm{BS}}_{\mathrm{pole}}(\mathbf{p})$, Eqs. (2.39)–(2.41). Their explicit expressions are

$$\mathcal{R}_{\hat{O}}(\mathbf{p})\equiv\left(-i\frac{1}{6M_D}\sum_M\frac{1}{(p_1^2-m^2)^2}\frac{1}{(p_2^2-m^2)}\right.$$
$$\times\mathrm{Tr}[\bar{G}_M(\hat{p}_1+m)\hat{O}(\hat{p}_1+m)$$
$$\left.\times G_M(\hat{p}_2+m)]\frac{dp_0}{2\pi}\right)\Bigg|_{\mathrm{pole}}, \tag{4.2}$$

where $\hat{O}$ stands for either γ_μ or $\mathbf{1}$. Now instead of calculating the pole contributions in Eq. (4.2), we go back to the original definition of these averages, following Eqs. (2.30) and (2.31), namely,

$$\mathcal{R}_{\hat{O}}(\mathbf{p})=\left(\frac{(p_2^2-m^2)}{4M_Dw}\frac{1}{3}\sum_M\mathrm{Tr}[\bar{\Psi}_M\hat{O}\right.$$
$$\left.\times\Psi_M(\hat{p}_2-m)]\right)\Bigg|_{p_0=M_D/2-E_2}, \tag{4.3}$$

and calculate directly the trace (4.3) evaluated at $p_0=M_D/2-E_2$. Here it is worth emphasizing that in our case, when

one particle (the second one in the present notation) is on-mass shell, only four partial amplitudes contribute to the process [13], namely, only those partial amplitudes (4.1) with the second ρ-spin index positive, i.e., the ${}^3S_1^{++}$, ${}^3D_1^{++}$, ${}^1P_1^{-+}$, and ${}^3P_1^{-+}$ amplitudes. In correspondence to these contributions, we introduce the Bethe-Salpeter wave functions for each vertex, viz.

$$\Psi_S(p_0,|\mathbf{p}|)=\frac{1}{\sqrt{2}\pi}\frac{G_S^{++}(p_0,|\mathbf{p}|)/2\pi}{\sqrt{2M_D}(2E_2-M_D)};$$

$$\Psi_D(p_0,|\mathbf{p}|)=\frac{1}{\sqrt{2}\pi}\frac{G_D^{++}(p_0,|\mathbf{p}|)/2\pi}{\sqrt{2M_D}(2E_2-M_D)}; \tag{4.4}$$

$$\Psi_{P_1}(p_0,|\mathbf{p}|)=\frac{1}{\sqrt{2}\pi}\frac{G_{^1P_1}^{-+}(p_0,|\mathbf{p}|)/2\pi}{\sqrt{2M_D}M_D};$$

$$\Psi_{P_3}(p_0,|\mathbf{p}|)=\frac{1}{\sqrt{2}\pi}\frac{G_{^3P_1}^{-+}(p_0,|\mathbf{p}|)/2\pi}{\sqrt{2M_D}M_D}, \tag{4.5}$$

where the normalization factors have been chosen so as to correspond to the nonrelativistic normalization of the deuteron wave function:

$$\int d\mathbf{p}(u^2(\mathbf{p})+w^2(\mathbf{p}))=1. \tag{4.6}$$

Then for $\mathcal{R}_{\hat{O}}$ we obtain

$$\mathcal{R}_{\gamma_0}=(2\pi)^3(\Psi_S^2(p_0,|\mathbf{p}|)+\Psi_D^2(p_0,|\mathbf{p}|)+\Psi_{P_1}^2(p_0,|\mathbf{p}|)+\Psi_{P_3}^2(p_0,|\mathbf{p}|)), \tag{4.7}$$

$$\mathcal{R}_{\vec{\gamma}}=(2\pi)^3\frac{\mathbf{p}}{E_2}(\Psi_S^2(p_0,|\mathbf{p}|)+\Psi_D^2(p_0,|\mathbf{p}|)-\Psi_{P_1}^2(p_0,|\mathbf{p}|)-\Psi_{P_3}^2(p_0,|\mathbf{p}|))+\delta\mathcal{R}_{\vec{\gamma}}, \tag{4.8}$$

$$\mathcal{R}_{\hat{\mathbf{1}}}=(2\pi)^3\frac{m}{E_2}(\Psi_S^2(p_0,|\mathbf{p}|)+\Psi_D^2(p_0,|\mathbf{p}|)-\Psi_{P_1}^2(p_0,|\mathbf{p}|)-\Psi_{P_3}^2(p_0,|\mathbf{p}|))+\delta\mathcal{R}_{\hat{\mathbf{1}}}, \tag{4.9}$$

where

$$\delta\mathcal{R}_{\vec{\gamma}}=(2\pi)^3\frac{\mathbf{p}}{E_2}\left\{\frac{2\sqrt{3}m}{3|\mathbf{p}|}[\Psi_S(p_0,|\mathbf{p}|)(\Psi_{P_1}(p_0,|\mathbf{p}|)-\sqrt{2}\Psi_{P_3}(p_0,|\mathbf{p}|))+\Psi_D(p_0,|\mathbf{p}|)(\sqrt{2}\Psi_{P_1}(p_0,|\mathbf{p}|)+\Psi_{P_3}(p_0,|\mathbf{p}|))]\right\}, \tag{4.10}$$

$$\delta\mathcal{R}_{\hat{\mathbf{1}}}=-(2\pi)^3\frac{m}{E_2}\left\{\frac{2\sqrt{3}|\mathbf{p}|}{3m}[\Psi_S(p_0,|\mathbf{p}|)(\Psi_{P_1}(p_0,|\mathbf{p}|)-\sqrt{2}\Psi_{P_3}(p_0,|\mathbf{p}|))+\Psi_D(p_0,|\mathbf{p}|)(\sqrt{2}\Psi_{P_1}(p_0,|\mathbf{p}|)+\Psi_{P_3}(p_0,|\mathbf{p}|))]\right\}. \tag{4.11}$$

As a conclusion, the inclusive eD cross section will be given by Eq. (2.38) with Eqs. (2.39)–(2.41) for $\langle\hat{1}\rangle^{\mathrm{BS}}$ and $\langle\gamma_\mu\rangle^{\mathrm{BS}}$ replaced by Eqs. (4.7)–(4.11).

From what we have exhibited, it can be seen that in the BS formalism, there is no universal momentum distribution [cf. Eqs. (4.7)–(4.9)] so that, in principle, a factorized cross section in the form (2.45) does not hold. This is a consequence of the covariance of the BS formalism, where the small components (4.5) with negative relative energies are taken into account. It has been shown [18] that the contribution from the waves with positive relative energies are much larger than the one from $\Psi_P^2(p_0,|\mathbf{p}|)$, which therefore, can be disregarded. However, the corrections (4.10) and (4.11), resulting from the interference between large and small waves contribute both to the static and to the moving nucleon contribution to the eD cross section and, *a priori*, cannot be disregarded; accordingly they will be taken into account in our calculations. Let us now introduce the following quantity, which will be called hereafter *the covariant relativistic momentum distribution*:

$$N^{\mathrm{BS}}(p_0,\mathbf{p})=N(p_0,\mathbf{p})+\delta N(p_0,\mathbf{p}), \tag{4.12}$$

where

$$N(p_0,\mathbf{p})=(\Psi_S^2(p_0,|\mathbf{p}|)+\Psi_D^2(p_0,|\mathbf{p}|)), \tag{4.13}$$

$$\delta N(p_0,\mathbf{p})=\left\{\frac{2\sqrt{3}}{3}[\Psi_S(p_0,|\mathbf{p}|)(\Psi_{P_1}(p_0,|\mathbf{p}|)-\sqrt{2}\Psi_{P_3}(p_0,|\mathbf{p}|))+\Psi_D(p_0,|\mathbf{p}|)(\sqrt{2}\Psi_{P_1}(p_0,|\mathbf{p}|)+\Psi_{P_3}(p_0,|\mathbf{p}|))]\right\}. \tag{4.14}$$

Since the relative energy p_0 is fixed, the momentum distribution (4.13), which is defined only in terms of the S and D components, resembles the nonrelativistic distribution $n_D(\mathbf{p})$, and therefore it is expected to provide the main contribution to the eD cross section.

Thus the matrix elements $\mathcal{R}_{\hat{O}}$, Eqs. (4.7)–(4.9), can be written in the following way:

$$\mathcal{R}_{\gamma_\mu}=(2\pi)^3\frac{p_\mu}{E_2}\cdot\begin{cases}N(p_0,\mathbf{p}), & \mu=0;\\ N(p_0,\mathbf{p})+\dfrac{m}{|\mathbf{p}|}\delta N(p_0,\mathbf{p}), & \mu=(1,2,3)\end{cases} \tag{4.15}$$

$$\mathcal{R}_{\hat{\mathbf{1}}}=(2\pi)^3\frac{m}{E_2}\cdot\left\{N(p_0,\mathbf{p})-\frac{|\mathbf{p}|}{m}\delta N(p_0,\mathbf{p})\right\}. \tag{4.16}$$

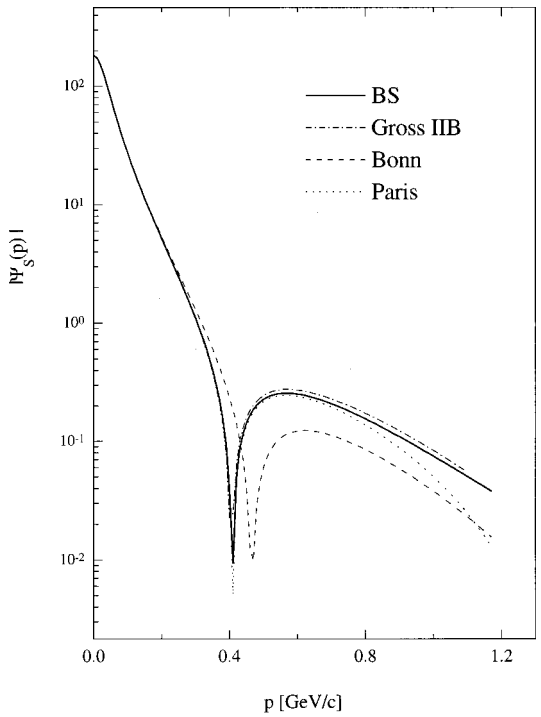

FIG. 12. The Bethe-Salpeter S wave $|\Psi_S(p_0,|\mathbf{p}|)|$ (solid line), with $p_0=M_D/2-\sqrt{\mathbf{p}^2+m^2}$, compared with the Gross S wave corresponding to the solution II B of Ref. [13] (dot-dashed) and with the nonrelativistic deuteron S wave obtained from the Paris (dotted) and Bonn (dashed) potentials.

If, for the time being, the quantity $\delta N(p_0,\mathbf{p})$ is disregarded, it is possible to relate the BS inclusive eD cross section to the elastic eN cross section for a moving nucleon; as a matter of fact, by inserting Eqs. (4.15) and (4.16) into Eqs. (2.39)–(2.41), one obtains

$$\left(\frac{d\sigma}{d\mathcal{E}'d\Omega_{k'}}\right)^{\rm BS}_{eD}=(2\pi)\int_{|y|}^{p_{\max}}|\mathbf{p}|d|\mathbf{p}|N(p_0,\mathbf{p}) \times\frac{E_{\vec{p}+\vec{q}}}{|\mathbf{q}|}(\tilde{\sigma}_{ep}+\tilde{\sigma}_{en}). \tag{4.17}$$

At large values of $|\mathbf{q}|$, Eq. (4.17) becomes

$$\left(\frac{d\sigma}{d\mathcal{E}'d\Omega_{k'}}\right)^{\rm BS}_{eD}\approx\{s_{ep}+s_{en}\}\frac{E_{|\vec{q}|+y}}{|\mathbf{q}|}(2\pi)\int_{|y|}^{\infty}|\mathbf{p}|d|\mathbf{p}|N(p_0,\mathbf{p}), \tag{4.18}$$

where, as before, $\tilde{\sigma}^{eN}$ and $E_{\vec{p}+\vec{q}}$ have been evaluated at $|\mathbf{p}|=|\mathbf{p}_{\min}|=|y|$. If Eq. (4.18) is placed in Eq. (3.5), the BS asymptotic scaling function is obtained, viz.

$$f^{\rm BS}(y)\equiv\frac{|\mathbf{q}|}{E_{y+|\vec{q}|}}\left(\frac{d\sigma}{d\mathcal{E}'d\Omega_{k'}}\right)^{\rm BS}_{eD}\{s_{ep}+s_{en}\}^{-1} =(2\pi)\int_{|y|}^{\infty}|\mathbf{p}|d|\mathbf{p}|\mathrm{N}(p_0,\mathbf{p}), \tag{4.19}$$

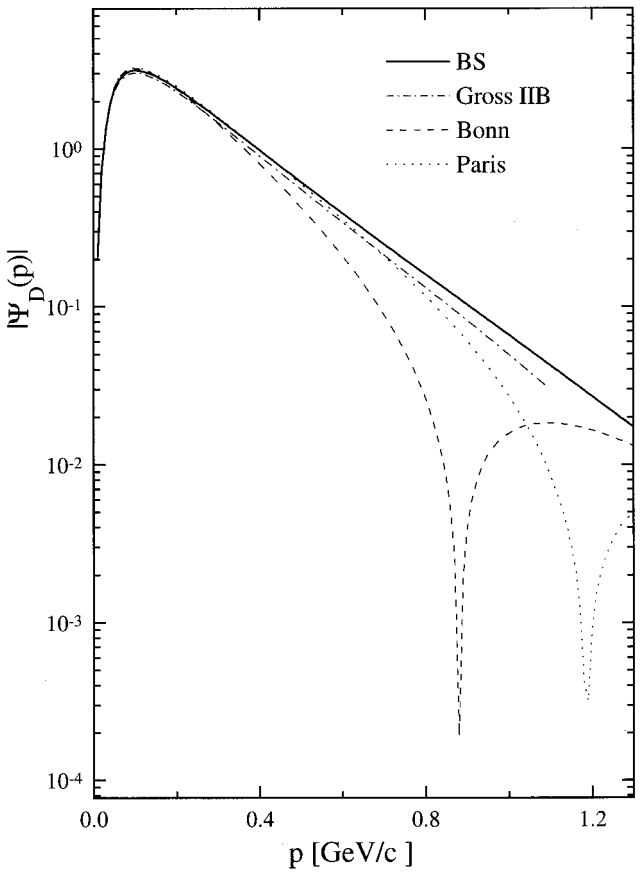

FIG. 13. The same as in Fig. 12 for the deuteron D wave.

from which information on the covariant nucleon momentum distribution $N(p_0,\mathbf{p})$ could be obtained.

The asymptotic scaling function, calculated by Eq. (4.19), coincides with the exact scaling function [obtained using Eqs. (2.38)–(2.41) in Eq. (3.5)] in the whole range of y (the

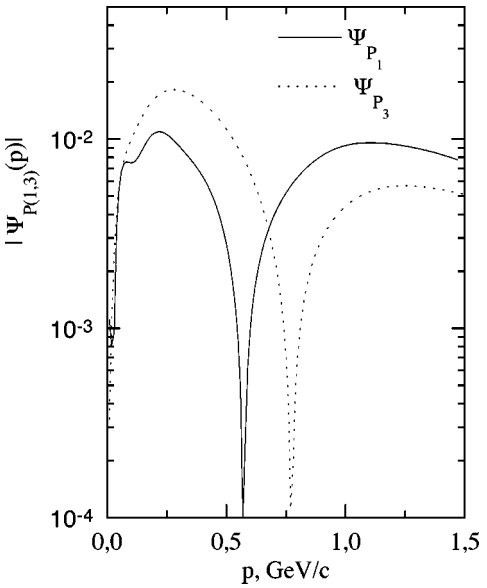

FIG. 14. The Bethe-Salpeter negative relative energy waves $\Psi_{P_{1,3}}(p_0,|\mathbf{p}|)$.

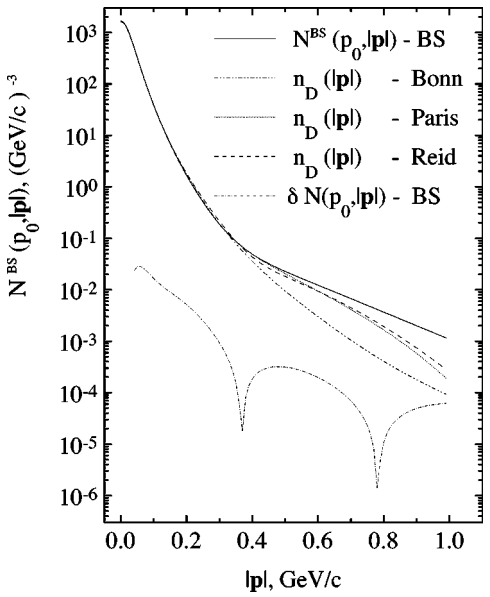

FIG. 15. The Bethe-Salpeter covariant momentum distribution (4.12), with $p_0 = M_D/2 - \sqrt{\mathbf{p}^2 + m^2}$, (full) and the contribution due to negative relative energy states (4.14) (dot-dashed). The nonrelativistic momentum distributions corresponding to the Bonn (dot-dot-dashed), Paris (dotted), and Reid (dashed) potentials are also shown.

largest difference occurring at $y = -0.8$ and being less than 10%), which means that the BS inclusive cross section could be safely replaced by its approximation (4.18). In order to understand such a result, in Figs. 12–14 the separate BS waves, viz. the S and D waves (full lines of Figs. 12 and 13), and the P_1 and P_3 waves (Fig. 14) are shown. It can be seen that the latter waves are smaller by order of magnitudes than the S and D waves, so that the quantity $\delta N(p_0, \mathbf{p})$, due to the interference terms (4.10) and (4.11) generated by the negative energy states, turns out to be negligible up to $|\mathbf{p}| \sim 1$ GeV/c. Thus we can conclude that in the interval $0 < |\mathbf{p}| < 1$ GeV/c the total distribution (4.12) can be safely approximated by the diagonal contribution (4.13), as illustrated in Fig. 15, where the full momentum distributions are shown. This is the reason why the BS inclusive cross section factorizes in the same way as the nonrelativistic one, and the relativistic scaling function (3.5) scales in y. In Figs. 12–15 we have also compared the full BS results with the results from other approaches, viz. the nonrelativistic Schrödinger approach with different types of interactions (see also Ref. [18]), as well as the relativistic approach based upon the Gross equations [13]. The BS and the Gross ([13]) approaches differ both in the form of the relativistic equations as well as in the number of exchanged bosons considered in the kernel (six in the former approach and four in the latter one), but both reproduce equally well the experimental NN phase shifts and the ground-state properties of the deuteron, which is reflected in the very similar behavior of the S and D waves shown in Figs. 12 and 13; these results also show that the high momentum content ($|\mathbf{p}| \simeq 0.5$ GeV/c) generated by relativistic equation is appreciably higher than the one provided by nonrelativistic wave functions.

V. SUMMARY AND CONCLUSIONS

In the present paper the inclusive quasielastic electron-deuteron cross section has been analyzed within the relativistic impulse approximation using recent, realistic solutions [21] of the spinor-spinor Bethe-Salpeter equation for the deuteron, with the interaction kernel including the exchange of π, σ, ω, ρ, η, and δ mesons. In our approach, both the $\gamma^* N$ and the $D \rightarrow NN$ vertices are treated relativistically, with eight components for the deuteron amplitude, unlike the usual, nonrelativistic approach [5], in which the $\gamma^* N$ is described by a relativistic free electron-nucleon cross section, and the $D \rightarrow NN$ vertex by the usual nonrelativistic two-component Schrödinger wave function (we reiterate that when we refer to the latter approach as the ''nonrelativistic'' one, we refer only to the $D \rightarrow NN$ vertex). The aim of our paper was twofold, viz.: (i) to investigate the relevance of relativistic effects, and (ii) to understand whether the concept of y scaling can be introduced in a relativistic description of inclusive eD scattering. The main results of our analysis can be summarized as follows:

(1) The relativistic inclusive eD cross section has been obtained in terms of the pole matrix elements $\langle \hat{\mathbf{1}} \rangle^{\rm BS}_{\rm pole}(|\mathbf{p}|)$ and $\langle \gamma_\mu \rangle^{\rm BS}_{\rm pole}(|\mathbf{p}|)$, taking into account the off-mass shellness of the nucleon and it has been found that unlike the nonrelativistic case, the BS cross section does not factorize into a product of the free electron-nucleon cross section and a structure factor depending upon the deuteron momentum distribution.

(2) It has been shown that the BS cross section can be written as a function of the three momentum transfers $\mathbf{q}$ and a variable y, which is exactly the same relativistic scaling variable used in the nonrelativistic approach and resulting from the relativistic instant-form energy-momentum conservation. Thus, in full analogy with the nonrelativistic case, a relativistic scaling function $F^{\rm BS}(|\mathbf{q}|, y)$ has been defined as the ratio of the BS eD cross section to the free eN cross section (times a proper phase space factor), and y scaling of $F^{\rm BS}(|\mathbf{q}|, y)$ has been demonstrated to occur, i.e., $F^{\rm BS}(|\mathbf{q}|, y) \rightarrow f^{\rm BS}(y)$, with the conditions for relativistic y scaling being very similar to those of nonrelativistic scaling, i.e., $2m/3 \leqslant \nu < |\mathbf{q}|$, $|\mathbf{q}| \geqslant 2m$.

(3) It has been pointed out that whereas the mechanism of nonrelativistic scaling is easily understood in terms of the rapid decay of the momentum distribution $n_D(\mathbf{p})$, which makes the nonrelativistic scaling function $F^{\rm NR}(|\mathbf{q}|, y) \sim 2\pi \int_{|y|}^{|\mathbf{q}|} n(\mathbf{p}) |\mathbf{p}| d|\mathbf{p}|$ to rapidly saturate with $|\mathbf{q}|$, i.e., to scale in y, a similar explanation in the relativistic case is not, in principle, possible, since, as stated in point 1, the BS cross section does not factorize, and, moreover, the concept of momentum distribution in the BS case is not uniquely defined. Thus, in order to understand the mechanism of the observed relativistic y scaling, the role of the various components of the BS amplitude was analyzed, and it has been found that if the extremely small diagonal contribution of the negative energy P waves is omitted, it is possible to define a covariant momentum distribution of the form $N^{\rm BS}(p_0, \mathbf{p}) = N(p_0, \mathbf{p}) + \delta N(p_0, \mathbf{p})$, where $\delta N(p_0, \mathbf{p})$, which originates from the interference between the positive and negative waves, can be safely disregarded provided $|\mathbf{p}| < 1$ GeV/c, so

that, as a result, the BS cross section factorizes in the same way as does the nonrelativistic cross section and the relativistic scaling function becomes $F^{\rm BS}(|\mathbf{q}|,y) \sim 2\pi \int_{|y|}^{|\mathbf{q}|} N(p_0,\mathbf{p})|\mathbf{p}|,d|\mathbf{p}|$; such a result provides the explanation for the relativistic y scaling and makes it possible to obtain the BS covariant momentum distributions by a simple first-order derivative of the asymptotic BS scaling function $f^{\rm BS}(y) \sim 2\pi \int_{|y|}^{\infty} N(p_0,\mathbf{p})\mathbf{p}|d|\mathbf{p}|$.

(4) The BS relativistic momentum distribution, $N(p_0,\mathbf{p})$, and the nonrelativistic one, $n_D(\mathbf{p})$, are practically the same up to $|\mathbf{p}| \sim 0.4$–0.5 GeV/c, where they start to differ by an amount which depends upon the two-body interaction producing $n_D(\mathbf{p})$. To sum up, it can be concluded that, if the effects from negative energy P states can be disregarded, which has been demonstrated to be the case when the nucleon momentum in the deuteron $|\mathbf{p}| \leqslant 1$ GeV/c, the concept of y scaling can be introduced in the BS relativistic description of inclusive quasielastic eD scattering, in the same way as it is in the conventional nonrelativistic approach, i.e., by introducing a scaling function which, in the scaling regime, is nothing but the nucleon longitudinal momentum distribution; moreover, both in the relativistic and nonrelativistic cases, scaling is shown to occur in the same variable y, and at values of ν and $|\mathbf{q}|$ such that quasielastic scattering is the dominant process.

ACKNOWLEDGMENTS

C.d.A. is very grateful to F. Gross for supplying us with the numerical values of the wave functions shown in Figs. 12 and 13. L.P.K. and A.Yu.U. are indebted to INFN, Sezione di Perugia, for warm hospitality and financial support. This work was partially supported by RFBR Grant No. 96-15-96423.

APPENDIX A: CONSTRUCTION OF THE NUCLEON OPERATOR

The contraction of the operators (2.16)–(2.19) with the leptonic tensor (2.13) yields

$$\hat{O}(p_1,q,k) \equiv \hat{O}_{\mu\nu}(p_1,q) L^{\mu\nu}(k,q) \tag{A1}$$

$$= \Bigg\{ F_1^2(Q^2)\hat{O}^{(1)}(p_1,q,k) + \frac{\kappa}{2m} F_1(Q^2)F_2(Q^2)\hat{O}^{(12)}(p_1,q,k) + \frac{\kappa^2}{4m^2} F_2^2(Q^2)\hat{O}^{(2)}(p_1,q,k) \Bigg\} \tag{A2}$$

$$\times (2\pi)\delta((p_1+q)^2-m^2), \tag{A3}$$

where

$$\hat{O}^{(1)}(p_1,q,k) = 2[q^2 m - \hat{q}(q^2+2kp_1) + \hat{k}(4kp_1 - 2qp_1)], \tag{A4}$$

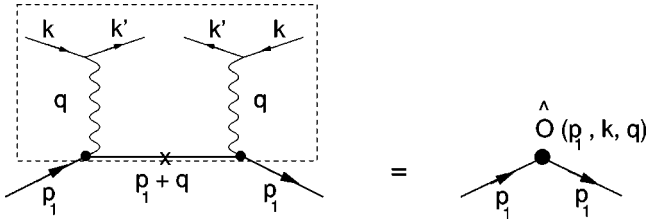

FIG. 16. The diagram defining the squared invariant matrix element for the deuteron in terms of the operator $\hat{O}$, Eq. (A1). The crossed line corresponds to the nucleon on the mass shell.

$$\hat{O}^{(12)}(p_1,q,k) = 4q^2[(-m\hat{q} + (q^2+qp_1))], \tag{A5}$$

$$\hat{O}^{(2)}(p_1,q,k) = 2q^2[mq^2 - \hat{q}(q^2+2qp_1-2kp_1) - 2\hat{k}(2kp_1 - qp_1)]. \tag{A6}$$

The average of Eq. (A6) with the nucleon or the deuteron amplitudes, times the factor e^2/Q^4, gives the invariant matrix elements.

A graphical representation of the operator $\hat{O}(p_1,q,k)$ is presented in Fig. 16, where the crossed nucleon line corresponds to a nucleon on the mass shell with the propagator $(2\pi)\delta((p_1+q)^2-m^2)(\hat{p}_1+\hat{q}+m)$.

The nucleon operator $\hat{O}(p_1,q,k)$ is the central object in our discussion about the connection between the nucleon and the deuteron cross sections. Let us first consider the differential elastic cross section for the process $e+N \to e'+N$. The invariant matrix element is defined by

$$|\mathcal{M}_{e+N\to e'+N}|^2 (2\pi)\delta((p_1+q)^2-m^2) = \frac{e^4}{Q^4}\frac{1}{2}\sum_{s_1} \langle p_1,s_1|\hat{O}(p_1,q,k)|p_1,s_1\rangle \tag{A7}$$

$$= \frac{e^4}{Q^4}\frac{1}{2}\mathrm{Tr}\{(\hat{p}_1+m)\hat{O}(p_1,q,k)\}. \tag{A8}$$

Let us first obtain the cross section in the rest frame of the nucleon $[p_1=(m,\mathbf{0})]$

$$\frac{1}{2}\mathrm{Tr}\{(\hat{p}_1+m)\hat{q}\} = 2m\nu, \quad \frac{1}{2}\mathrm{Tr}\{(\hat{p}_1+m)\hat{k}\} = 2m\mathcal{E},$$

$$\frac{1}{2}\mathrm{Tr}\{(\hat{p}_1+m)\} = 2m, \tag{A9}$$

$$kp_1 = m\mathcal{E}, \quad qp_1 = m\nu, \tag{A10}$$

so that

$$|\mathcal{M}_{e+N\to e'+N}|^2(2\pi)\delta((p_1+q)^2-m^2)$$

$$=\frac{e^4}{Q^4}[4(m^2q^2-m\nu q^2-4m^2\nu\mathcal{E}+4m^2\mathcal{E}^2)F_1^2(Q^2)+4\kappa q^4F_1(Q^2)F_2(Q^2)$$

$$+\kappa^2q^2(q^2-4\mathcal{E}^2+4\nu\mathcal{E})F_2^2(Q^2)](2\pi)\delta(2m\nu-Q^2) \tag{A11}$$

$$=\frac{e^4}{Q^4}16m^2\mathcal{E}\mathcal{E}'\left[\left(\cos^2\frac{\theta}{2}-\frac{q^2}{2m^2}\sin^2\frac{\theta}{2}\right)F_1^2(Q^2)-\frac{\kappa q^2}{m^2}\sin^2\frac{\theta}{2}F_1(Q^2)F_2(Q^2)-\frac{\kappa^2q^2}{4m^2}\left(1+\sin^2\frac{\theta}{2}\right)F_2^2(Q^2)\right]$$

$$\times(2\pi)\delta(2m\nu-Q^2) \tag{A12}$$

$$=\frac{e^4}{Q^4}16m^2\mathcal{E}\mathcal{E}'\left[\cos^2\frac{\theta}{2}\left(F_1^2(Q^2)-\frac{\kappa^2q^2}{4m^2}F_2^2(Q^2)\right)-\frac{q^2}{2m^2}\sin^2\frac{\theta}{2}\,(F_1(Q^2)+\kappa F_2(Q^2))^2\right](2\pi)\delta(2m\nu-Q^2). \tag{A13}$$

Inserting the last expression in Eq. (2.11) we get the Rosenbluth cross section:

$$\frac{d\sigma}{d\mathcal{E}'\,d\Omega_{k'}}=\frac{\alpha^2m}{2\mathcal{E}^2\sin^4(\theta/2)}\left[\cos^2\frac{\theta}{2}\left(F_1^2(Q^2)-\frac{\kappa^2q^2}{4m^2}F_2^2(Q^2)\right)-\frac{q^2}{2m^2}\sin^2\frac{\theta}{2}(F_1(Q^2)+\kappa F_2(Q^2))^2\right]\delta(2m\nu-Q^2) \tag{A14}$$

$$=\sigma_{\rm Mott}\left[\left(F_1^2(Q^2)-\frac{\kappa^2q^2}{4m^2}F_2^2(Q^2)\right)-\frac{q^2}{2m^2}\tan^2\frac{\theta}{2}(F_1(Q^2)+\kappa F_2(Q^2))^2\right]\delta\left(\nu-\frac{Q^2}{2m}\right). \tag{A15}$$

Let us now consider the eD cross section. To this end, we will consider an arbitrary reference frame where the four momentum of the nucleon is $p_1=(p_{10},\mathbf{p}_1)$; moreover the nucleon can be off-mass shell ($p_1^2\neq m^2$).

Our strategy now is to explicitly separate that part of the operator describing the free nucleon at rest, i.e., the part defining the cross section (A15), from the remaining parts of the operator due to the nucleon motion and the off-mass-shell corrections.

Rearranging the terms in Eqs. (A1)–(A6) according to their contributions, we find

$$\hat{O}(p_1,q,k)=\{\hat{O}_{\rm on}+\delta\hat{O}_{\rm off}\}(2\pi)\delta((p_1+q)^2-m^2), \tag{A16}$$

where $\hat{O}_{\rm on}$ is the sum of terms contributing to the invariant matrix element for the free nucleon, and $\delta\hat{O}_{\rm off}$ is the sum of the terms providing the off-mass-shell corrections. Since we can add to and subtract from both terms in Eq. (A16) pieces vanishing for a nucleon on the mass shell, the separation on $\hat{O}_{\rm on}$ and $\delta\hat{O}_{\rm off}$ is not unique, but the physical results do not depend on the way this is done. In our definition

$$\hat{O}_{\rm on}\equiv\frac{q^4}{m}B(Q^2)+2[q^2m-2\hat{q}(kp_1)$$

$$+2\hat{k}(2kp_1-qp_1)]A(Q^2), \tag{A17}$$

$$\delta\hat{O}_{\rm off}\equiv-2q^2\left(\hat{q}+\frac{q^2}{2m}\right)F_1^2(Q^2)$$

$$+\frac{2\kappa q^2}{m}(-m\hat{q}+qp_1)F_1(Q^2)F_2(Q^2)$$

$$-\frac{\kappa^2q^2}{2m^2}[\hat{q}(q^2+2qp_1)]F_2^2(Q^2). \tag{A18}$$

It can be seen that in Eq. (A17) $A(Q^2)$ and $B(Q^2)$ are weighted by two different functions, viz. a scalar, and a mixture of scalar and vector terms, respectively. This is a result of the relativistic structure of our formalism, in which, unlike the nonrelativistic case and the relativistic case for a nucleon at rest, the vector charge density does not coincide with the probability density. Because of the different structure of the weighting factors of $A(Q^2)$ and $B(Q^2)$ in $\hat{O}_{\rm on}$, the average value of the latter calculated for the deuteron will not factorize into a common term for $A(Q^2)$ and $B(Q^2)$. However, if the difference between the vector and the scalar charges is not too large, one could be able to define a common term for both $A(Q^2)$ and $B(Q^2)$, plus proper correction terms. Therefore, we redefine our definition of $\hat{O}_{\rm on}$:

$$\hat{O}_{\rm on}\equiv\hat{O}_{\rm stat}+\delta\hat{O}_{\rm mot}, \tag{A19}$$

$$\hat{O}_{\rm stat}=2[q^2m-4m\nu\mathcal{E}+4m\mathcal{E}^2]A(Q^2)+\frac{q^4}{m}B(Q^2), \tag{A20}$$

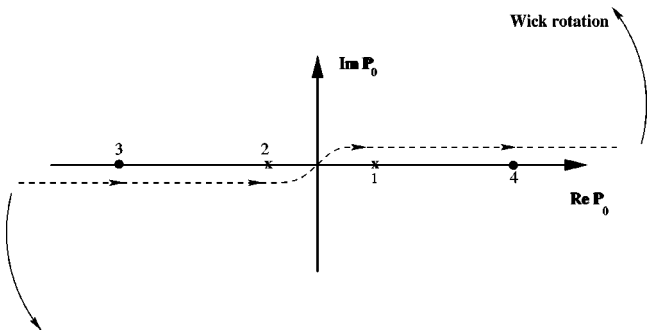

FIG. 17. The integration contour in Eq. (B2). The singularities 1 and 2 correspond to the first and second particles on-mass shell, $p_{10}=w$ and $p_{20}=w$, respectively, whereas the singularities labeled as 3 and 4 correspond to both particles off-mass shell, $p_{10}=-w$ and $p_{20}=-w$.

$$\delta\hat{O}_{\rm mot}=4[m\nu\mathcal{E}-\hat{q}(kp_1)-\mathcal{E}(2m\mathcal{E}-m\nu)+\hat{k}(2kp_1-qp_1)]A(Q^2), \tag{A21}$$

where $\hat{O}_{\rm stat}$ is a scalar operator defining the invariant matrix element for the nucleon at rest and $\delta\hat{O}_{\rm mot}$ is defined by the combination of scalar and vector currents, which gives a nonzero contribution for the moving nucleon.

APPENDIX B: THE POLE STRUCTURE OF THE MATRIX ELEMENTS WITHIN THE BS FORMALISM

In computing the deuteron observables within the BS formalism, i.e., the matrix elements of a given operator $\langle D|\hat{O}|D\rangle\equiv\langle\hat{O}\rangle$, one makes use of the Mandelstam technique, which yields

$$\langle\hat{O}\rangle=\frac{i}{2M_D}\int\frac{d^4p}{(2\pi)^4}\frac{1}{(p_1^2-m^2+i\epsilon)^2(p_2^2-m^2+i\epsilon)}\times\frac{1}{3}\sum_M \mathrm{Tr}\{\bar{G}_M(p_0,\mathbf{p})(\hat{p}_1+m)\hat{O}(\hat{p}_1+m)\times G_M(p_0,\mathbf{p})(\hat{p}_2+m)\}. \tag{B1}$$

It can be seen that in Eq. (B1) there are poles and cuts in the integration over p_0. However, the whole matrix element $\langle\hat{O}\rangle$ is real and finite. This allows one to perform the Wick rotation in the complex plane of the relative energy p_0 and safely compute the integrals in Eq. (B1). Moreover, in this case the BS vertex function $G_M(p_0,\mathbf{p})$ depends upon the imaginary part of p_0, which allows one to use directly the numerical solution [21,20] obtained in the rotated system. In particular, when $\langle\hat{O}\rangle$ is defined at fixed value of p_0 (which is just the case of eD processes investigated in this paper) the Wick rotation is no longer relevant in the computation of matrix elements. In order to establish a connection between the calculation of matrix elements in the form of Eq. (B1) and the matrix elements (2.30), we introduce the deuteron densities (see also Ref. [31]):

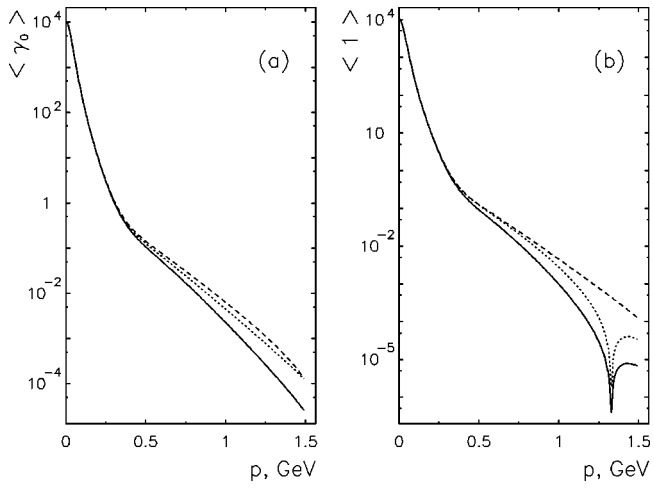

FIG. 18. The deuteron densities: (a) $\langle\gamma_0\rangle(|\mathbf{p}|)$. The solid line corresponds to the integration over p_0, and the dashed line to the nucleon pole contribution; the nucleon pole contribution to the scalar density $\langle 1\rangle(|\mathbf{p}|)$ is given by the dotted line. (b) $\langle 1\rangle(|\mathbf{p}|)$. The solid line corresponds to the integration over p_0 and the dashed line to the nucleon pole contribution; the dotted line represents the nucleon pole contribution to the scalar density calculated via $\langle\gamma_0\rangle(|\mathbf{p}|)[1-\mathbf{p}^2/(2m^2)]$.

$$\langle\hat{O}\rangle^{\rm BS}(\mathbf{p})=\frac{i}{2M_D}\int\frac{dp_0}{(2\pi)}\frac{1}{(p_1^2-m^2+i\epsilon)^2(p_2^2-m^2+i\epsilon)}\times\frac{1}{3}\sum_M \mathrm{Tr}\{\bar{G}_M(p_0,\mathbf{p})(\hat{p}_1+m)\times\hat{O}(\hat{p}_1+m)G_M(p_0,\mathbf{p})(\hat{p}_2+m)\}, \tag{B2}$$

where the integration contour is shown in Fig. 17. There are two kinds of singularities in Eq. (B2): (i) when one of the particles is on mass shell, $p_{10}=w$ or $p_{20}=w$, labeled ''1'' and ''2'' in Fig. 17, and (ii) when both particles are deeply virtual, $p_{10}=-w$ or $p_{20}=-w$, labeled ''3'' and ''4,'' respectively. As previously mentioned, in Eq. (B2) the singularities are removed by performing the Wick rotation and by integrating along the imaginary axis of p_0. Instead of rotating the contour, we close it in the upper semiplane, and integrate Eq. (B2) in the Minkowsky space. Thus there remain two singularities contributing to the full densities, a simple pole at $p_{20}=w$, and a pole of second order at $p_{10}=-w$. The former, which corresponds to the spectator on the mass shell, gives the dominant contribution to the full integral. It is exactly this contribution which enters our formulas in Sec. II [Eq. (2.30)], and in Sec. III [Eqs. (2.39)–(2.41)]. The approximation of the full matrix elements by the nucleon pole contribution is often used in describing the processes with the deuteron [13,32]. Accordingly let us define the nucleon pole contribution to the full density:

$$\langle \hat{O} \rangle^{\mathrm{BS}}_{\mathrm{pole}}(\mathbf{p}) = \frac{1}{2M_D} \frac{1}{2wM_D^2(M_D-2w)^2} \frac{1}{3} \sum_M \mathrm{Tr}\{\overline{G}_M(p_0,\mathbf{p}) \times (\hat{p}_1+m)\hat{O}(\hat{p}_1+m)G_M(p_0,\mathbf{p})(\hat{p}_2+m)\}. \tag{B3}$$

It can be seen that the matrix element (2.30) is the pole part of Eq. (B1). Insofar as the pole contribution [Eq. (B3)] dominates the full density [Eq. (B2)], the relevant quantities [Eqs. (2.39)–(2.41)] can be calculated by using the Wick rotation and by computing numerically the integral (B2) in the rotated system, using the numerical solutions of the BS equation obtained in Ref. [21]. Figure 18 shows the charge $\langle \gamma_0 \rangle$ and scalar $\langle 1 \rangle$ densities computed by Eqs. (B2) and (B3). It can be seen that up to $|\mathbf{p}| \sim 0.65$ GeV/c, both methods provide the same results (above 0.65 GeV/c the pole contribution has been calculated using for the BS vertex function G_M, the analytical parametrization from Ref. [20]). More details on the behavior of various full and pole densities can be found in Ref. [31].

[1] J.D. Bjorken, Phys. Rev. **179**, 1547 (1969).
[2] G.B. West, Phys. Rep., Phys. Lett. **18C**, 264 (1975).
[3] L. Frankfurt and M. Strikman, Phys. Rep. **160**, 235 (1988).
[4] E. Pace and G. Salme, Phys. Lett. **110B**, 411 (1982).
[5] C. Ciofi degli Atti, E. Pace, and G. Salme, Phys. Rev. C **43**, 1155 (1991).
[6] D.B. Day, J.S. McCarthy, T.W. Donelly, and I. Sick, Annu. Rev. Nucl. Part. Sci. **40**, 357 (1990).
[7] I. Sick, D. Day, and J.S. McCarthy, Phys. Rev. Lett. **45**, 871 (1980).
[8] S. Rock *et al.*, Phys. Rev. Lett. **49**, 1139 (1982).
[9] C. Ciofi degli Atti, E. Pace, and G. Salme, Phys. Rev. C **36**, 1208 (1987).
[10] X. Ji and B. F. Filippone, Phys. Rev. C **42**, R2279 (1992); A. Bianconi, S. Jeshonnek, N.N. Nikolaev, and B.G. Zakharov, Phys. Lett. B **338**, 123 (1994); **363**, 217 (1995); L.L. Frankfurt, M. Sargsyan, and M.I. Strikman, Phys. Rev. C **56**, 1124 (1997); H. Morita, C. Ciofi degli Atti, and D. Treleani, nucl-th/9901086.
[11] W.N. Polyzou and W. Glökle, Phys. Rev. C **53**, 3111 (1996).
[12] B.D. Keister, Phys. Rev. C **37**, 1765 (1988).
[13] F. Gross, Phys. Rev. **186**, 1448 (1969); W.W. Buck and F. Gross, Phys. Rev. C **20**, 2361 (1979); F. Gross, J.W. Van Orden, and K. Holinde, *ibid.* **45**, 2094 (1992); J.W. Van Orden, N. Devine, and F. Gross, Phys. Rev. Lett. **75**, 4369 (1995).
[14] B. Desplanques, V.A. Karmanov, and J.F. Mathiot, Nucl. Phys. **A589**, 697 (1995).
[15] M.J. Zuilhof and J.A. Tjon, Phys. Rev. C **22**, 2369 (1980).
[16] J. Fleischer and J.A. Tjon, Nucl. Phys. **B84**, 375 (1975); Phys. Rev. D **15**, 2537 (1977).
[17] B.D. Keister and J.A. Tjon, Phys. Rev. C **26**, 578 (1982).
[18] L.P. Kaptari *et al.*, Phys. Rev. C **54**, 986 (1996).
[19] A. Yu. Umnikov and F.C. Khanna, Phys. Rev. C **49**, 2311 (1994); Mod. Phys. Lett. **10**, 91 (1995).
[20] A.Yu. Umnikov, Z. Phys. A **357**, 333 (1997).
[21] A.Yu. Umnikov, L.P. Kaptari, K.Yu. Kazakov, and F. Khanna, Phys. Lett. B **334**, 163 (1994).
[22] C. Ciofi degli Atti, D. Faralli, A. Yu. Umnikov and L.P. Kaptari (unpublished).
[23] T. de Forest, Jr., Nucl. Phys. **A392**, 232 (1983).
[24] S. Pollock, H.W.L. Naus, and J.H. Koch, Phys. Rev. C **53**, 2304 (1996); J. Kelly, *ibid.* **56**, 2672 (1997).
[25] H. Arenhövel, W. Liedemann, and E. Tomusiak, Phys. Rev. C **46**, 455 (1992); G. Beck and H. Arenhövel, Few-Body Syst. **13**, 165 (1992).
[26] C. Ciofi degli Atti, A. Yu. Umnikov, L.P. Kaptari, K.Yu. Kazakov, and S. Scopetta, Phys. Rev. C **51**, 52 (1995).
[27] R. Machleid, K. Holinde, and Ch. Elster, Phys. Rep. **149**, 1 (1987).
[28] M. Lacombe *et al.*, Phys. Rev. C **21**, 861 (1980).
[29] R.V. Reid, Jr., Ann. Phys. (N.Y.) **50**, 411 (1968).
[30] J.J. Cubis, Phys. Rev. D **6**, 547 (1972).
[31] A.Yu. Umnikov, F.C. Khanna, and L.P. Kaptari, Phys. Rev. C **56**, 1700 (1997).
[32] L.S. Celenza, C.M. Shakin, and W. Koepf, Phys. Rev. C **42**, 1989 (1990).